

Discovery of Novel pERK1/2- or β -Arrestin-Preferring 5-HT_{1A} Receptor-Biased Agonists: Diversified Therapeutic-like versus Side Effect Profile

Joanna Snieciakowska, Monika Gluch-Lutwin, Adam Bucki, Anna Więckowska, Agata Siwek, Magdalena Jastrzebska-Wiesek, Anna Partyka, Daria Wilczyńska, Karolina Pytka, Gniewomir Latacz, Katarzyna Przejczowska-Pomierny, Elżbieta Wyska, Anna Wesołowska, Maciej Pawłowski, Adrian Newman-Tancredi, and Marcin Kolaczowski*

Cite This: *J. Med. Chem.* 2020, 63, 10946–10971

Read Online

ACCESS |



Metrics & More

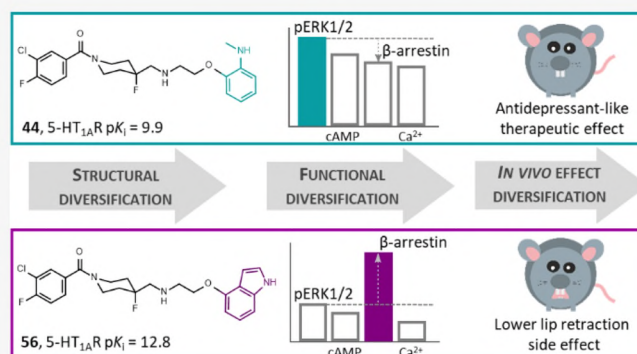


Article Recommendations



Supporting Information

ABSTRACT: Novel 1-(1-benzoylpiperidin-4-yl)methanamine derivatives with high affinity and selectivity for serotonin 5-HT_{1A} receptors were obtained and tested in four functional assays: ERK1/2 phosphorylation, adenylyl cyclase inhibition, calcium mobilization, and β -arrestin recruitment. Compounds **44** and **56** (2-methylaminophenoxyethyl and 2-(1*H*-indol-4-yloxy)ethyl derivatives, respectively) were selected as biased agonists with highly differential “signaling fingerprints” that translated into distinct *in vivo* profiles. *In vitro*, **44** showed biased agonism for ERK1/2 phosphorylation and, *in vivo*, it preferentially exerted an antidepressant-like effect in the Porsolt forced swimming test in rats. In contrast, compound **56** exhibited a first-in-class profile: it preferentially and potently activated β -arrestin recruitment *in vitro* and potentially elicited lower lip retraction *in vivo*, a component of “serotonergic syndrome”. Both compounds showed promising developability properties. The presented 5-HT_{1A} receptor-biased agonists, preferentially targeting various signaling pathways, have the potential to become drug candidates for distinct central nervous system pathologies and possessing accentuated therapeutic activity and reduced side effects.



INTRODUCTION

Although serotonin 5-HT_{1A} receptors exert a major influence on central nervous system (CNS) functions such as mood, pain, and movement and were identified several decades ago,^{1,2} it is notable that there are still no selective 5-HT_{1A} receptor agonists approved for therapeutic intervention. There are, of course, commercialized drugs that exhibit some agonist properties at 5-HT_{1A} receptors, including the anxiolytic buspirone (Buspar), the antidepressant vortioxetine (Brintellix), the antipsychotic aripiprazole (Abilify), and the antiparkinsonian bromocriptine (Parlodel).^{3–6} However, all of these compounds also interact with other targets, including other monoamine receptors or transporters, and they only partially activate 5-HT_{1A} receptors (*i.e.*, they function as “partial agonists”). Moreover, such compounds do not discriminate between subpopulations of 5-HT_{1A} receptors which are expressed in different brain regions and that mediate various, sometimes opposing, physiological and behavioral responses. For example, activation of postsynaptic 5-HT_{1A} heteroreceptors in the frontal cortex elicits procognitive and antidepressant effects, whereas activation of presynaptic

5-HT_{1A} autoreceptors is associated with prodepressive effects, notably by inhibiting the release of serotonin in terminal regions.^{7,8} These contrasting effects have long been the object of discussion in the search for more efficacious antidepressants and suggest that indiscriminate activation of multiple 5-HT_{1A} receptor subpopulations may limit the therapeutic efficacy of 5-HT_{1A} receptor agonists or elicit unacceptable side effects. In contrast, recent advances have shown that it is possible to selectively target 5-HT_{1A} receptors in desired brain areas, such as the cortex or brain stem, leading to significantly improved and promising therapeutic-like outcomes.

The basis for such preferential brain region targeting is the emerging concept of “biased agonism” at G-protein-coupled receptors. Accumulated studies in recent years provide

Received: May 13, 2020

Published: September 4, 2020



compelling evidence that different agonists can preferentially activate intracellular signaling *via* specific effectors, such as different G-protein subtypes or β -arrestins. Given that coupling to particular signaling mechanisms can vary from one brain region to another, this provides a basis for biased agonists to differentially activate particular brain regions. Such differential signaling may be associated with specific neurochemical, physiological, and behavioral responses and has been proposed in the context of drug discovery at a variety of receptor subtypes as a strategy to achieve superior therapeutic outcomes.^{9–11}

In the case of 5-HT_{1A} receptors, an important advance was the discovery of a first highly selective biased agonist, NLX-101 (aka F15599, **1**), which shows a marked preference for ERK1/2 phosphorylation versus other signaling pathways (Figure 1).^{12,13} **1** displayed a strikingly superior activity profile in a

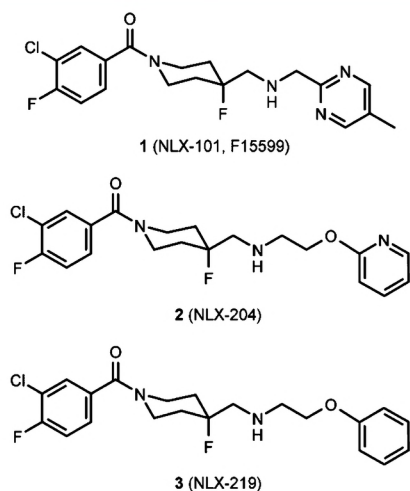


Figure 1. Selective 5-HT_{1A} receptor-biased agonists.

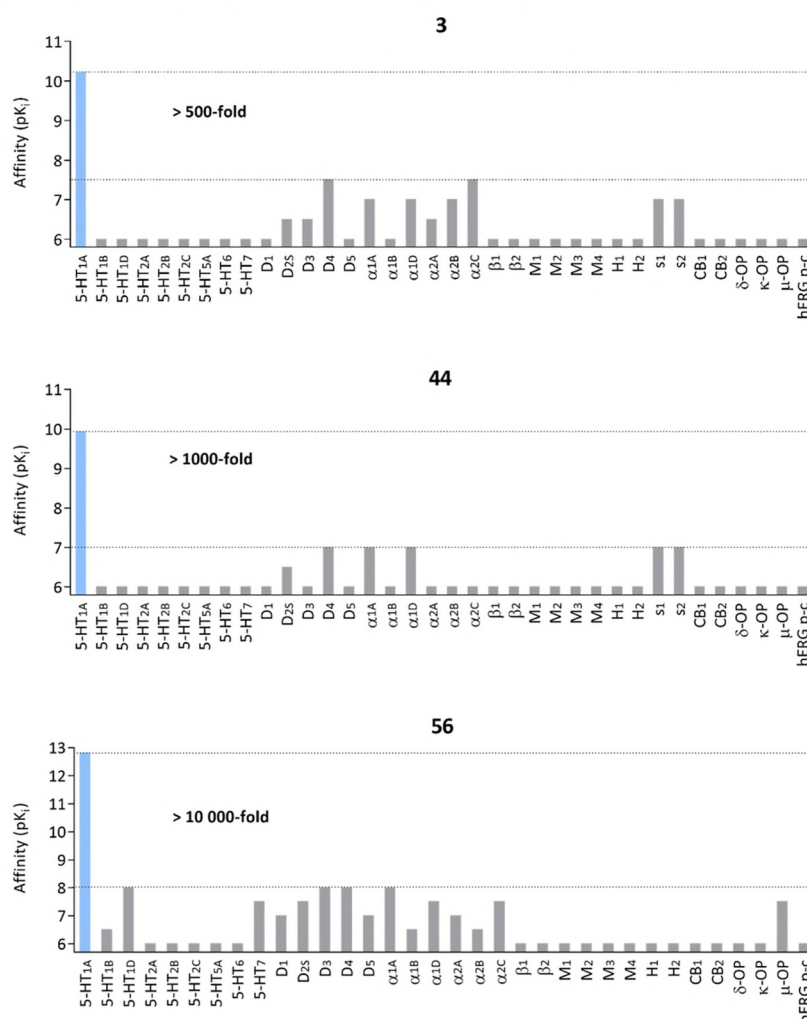
variety of electrophysiology, microdialysis, behavior, and brain imaging studies, as compared to older, canonical 5-HT_{1A} receptor agonists.^{14–16} In particular, **1** exhibited highly promising properties in models of antidepressant and procognitive activity as well as in models of respiratory deficits in Rett syndrome, an orphan disorder.^{17,18} The discovery of **1** therefore opened the way for drug discovery of novel, selective biased agonists that target 5-HT_{1A} receptors in specific brain areas that control CNS functions and that constitute, potentially, more efficacious and safer pharmacotherapeutics.

However, despite its broad pharmacological characterization, **1** remained isolated as a single example of a biased agonist with a superior pharmacological profile but with no medicinal chemistry data allowing for rational design of other functionally selective 5-HT_{1A} receptor agonists. In this context, our previous work investigated the structure–activity relationship (SAR) and structure functional activity relationships (SFARs) of novel analogues designed based on the structure of **1**.¹³ In that study, we identified a new, patentable, and synthetically versatile chemotype of selective 5-HT_{1A} receptor-biased agonists that preferentially activate ERK1/2 phosphorylation *in vitro* and show potent antidepressant-like properties *in vivo*. These findings met our objectives but did not identify structures that may exhibit other biased agonist profiles, notably for β -arrestin recruitment, which, as mentioned above, is a major target for G protein coupled receptor (GPCR)-biased agonist studies.

The present study builds upon the conclusion that the pyridine-2-oxy- or phenoxy-ethyl or derivatives of 1-(1-benzoylpiperidin-4-yl)methanamine, represented by lead structures **2** (NLX-204) and **3** (NLX-219), are the most promising chemotypes for obtaining new selective full agonists of the 5-HT_{1A} receptor (Figure 1). As our previous work studied various unsubstituted derivatives, we focused herein on determining the influence of the substitution pattern at the phenyl ring. Based on molecular modeling studies, we observed that phenyl moiety binds in the part of the receptor that is responsible for the stabilization of various bioactive conformations (between transmembrane helices 3, 5, and 6), thus justifying diversification of this fragment to obtain biased agonists with novel profiles of functional selectivity.^{13,19} Specifically, we aimed to obtain, on the one hand, agonists with higher levels of bias for specific signaling pathways (notably pERK1/2) and, on the other hand, agonists exhibiting bias for signaling pathways other than pERK1/2 (notably β -arrestin recruitment). Such biased agonists with diversified functional profiles could prove to be beneficial for different CNS disorders involving serotonergic dysregulation. A series of variously substituted phenoxyethyl derivatives of 1-(1-benzoylpiperidin-4-yl)methanamine was therefore synthesized and extensively tested in a stepwise manner to yield novel, selective, and functionally diversified 5-HT_{1A} receptor agonists. As well as broadening our knowledge about the pharmacology of 5-HT_{1A} receptors, such compounds could constitute promising candidates for treatment of different disorders involving serotonergic neurotransmission, some of which (such as depression) may be anticipated to respond to pERK1/2-biased agonists, whereas others may be better treated with β -arrestin-biased agonists. Overall, the availability of novel compounds differentially targeting these key signaling mechanisms raises the prospect of achieving increased therapeutic efficacy with reduced side effects in the treatment of CNS disorders.

RESULTS AND DISCUSSION

Design of a Novel Series of Variously Substituted Phenoxyethyl Derivatives of 1-(1-Benzoylpiperidin-4-yl)methanamine. In the present study, we decided to use compound **3**, a previously described unsubstituted phenoxyethyl derivative of 1-(1-benzoylpiperidin-4-yl)methanamine, as a lead structure for modifications. The previously assessed *in silico* developability measures for compound **3**, namely, CNS MPO = 4.89, LELP = 6.7 and Fsp3 = 0.38, were considered favorable.¹³ However, to further confirm the properties of this compound as a good lead structure, some *in vitro* studies were applied. They included metabolic stability using rat liver microsomes (RLMs), membrane permeability using parallel artificial membrane permeability assay (PAMPA), hepatotoxicity on HepG2 cell line, as well as extended selectivity study on a multitarget panel, including 45 receptors (for the sake of comparison between the lead structure and the most interesting derivatives developed within the present study, the abovementioned data for these compounds are collected in Table 7 and Chart 1 as well as Supporting Information Table S3). Compound **3** showed acceptable metabolic stability, high permeability, very low potential for hepatotoxicity, and significant (at least 500 \times) selectivity versus the off-targets, including the hERG channel, thus proving to be a good starting point for further modifications. The structural diversification was focused on introducing various substituents to the

Chart 1. Graphical Visualization of Selectivity Profiles of Compounds 3, 44, and 56^a

^aFor the sake of clarity, 34 most important targets are shown out of 46 tested. The pK_i values shown were estimated based on screening data and rounded to the nearest half-log value. For full selectivity data, see Supporting Information Tables S4 and S5. hERG p-c—hERG blockade determined using the patch-clamp method.

phenoxy moiety in order to modulate the functional profile while maintaining favorable developability. The choice of substituents was controlled primarily by molecular weight, number of hydrogen bond donors and lipophilicity, as well as synthetic feasibility of the final molecules. As a result, a set of 30 novel compounds was proposed for chemical synthesis and pharmacological evaluation.

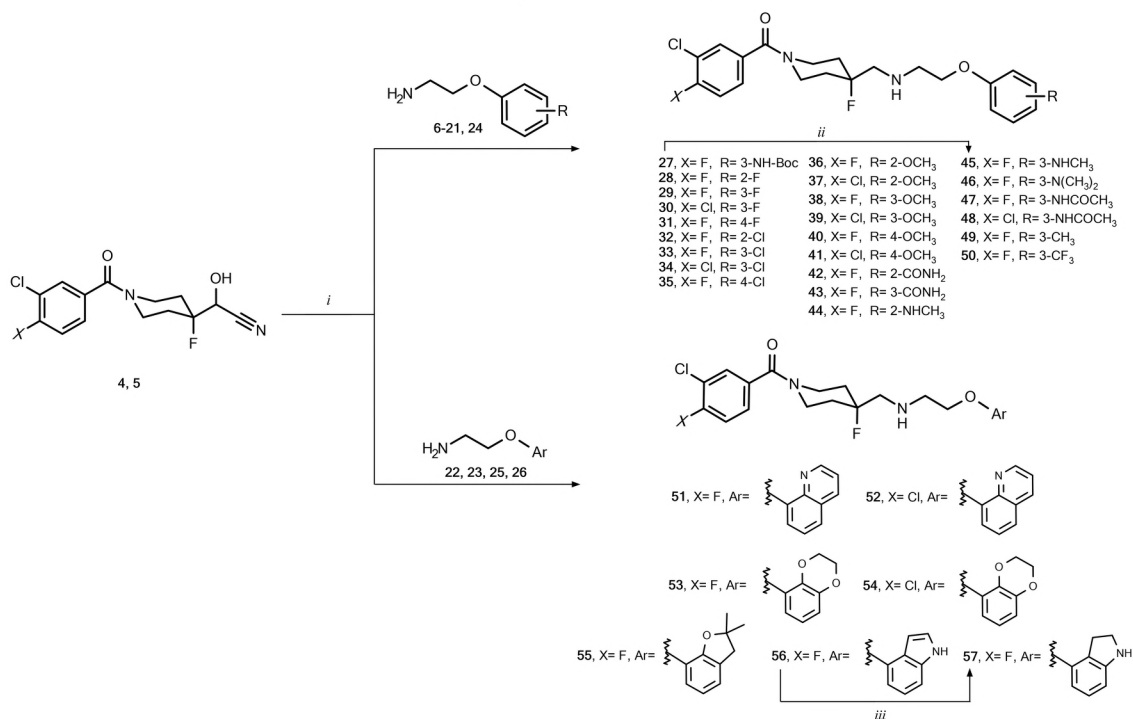
Synthesis. To prepare the target compounds 28–57, we have utilized a method that we have previously used and described (Scheme 1).¹³ The method is based on a reaction of reductive amination between cyanohydrins 4 or 5 and the appropriate amines (6–26). Briefly, cyanohydrins 4 and 5 were prepared in Darzens reaction from benzoylpiperidin-4-on derivatives and chloroacetonitrile, followed by a regioselective ring opening with poly(hydrogen fluoride)pyridine. Amines 6–26 were prepared from the corresponding phenols according to two synthetic pathways depicted in Scheme 2.

Amines 6–23 were synthesized according to a three-step procedure starting with Williamson reaction²⁰ using appropriate phenols and 1,2-dibromoethane. The obtained 2-bromoethoxy derivatives (I 6–23) were used in Gabriel's synthesis,^{21–23} leading to the desired primary amines. Syn-

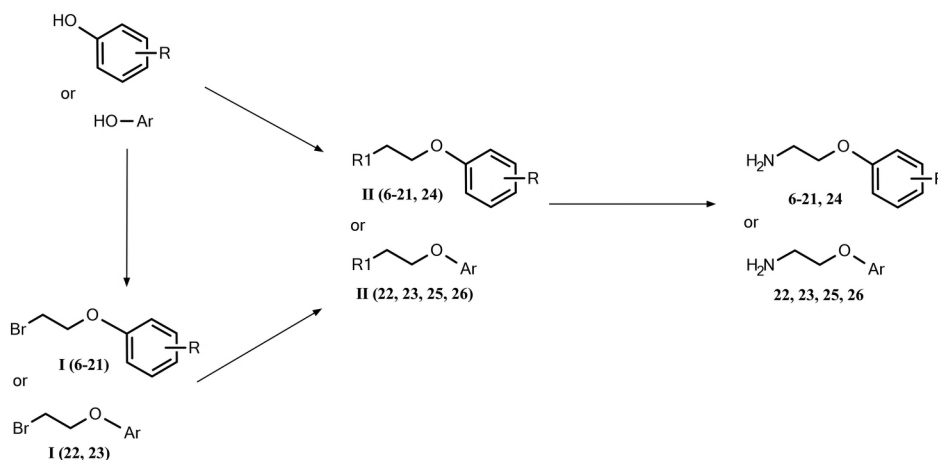
thesis of amine 17 (R = 3-NH-CH₃) required additional Boc-protection to prevent reductive amination at a secondary amine group. Deprotection of the amine was performed at the last step of the synthesis of compound 45 (Scheme 1). Amines 24–26 were obtained in Mitsunobu reaction^{24,25} of 2-(methylamino)phenol with *tert*-butyl-2-hydroxyethyl carbamate (II 24) and quinolin-8-ol or 1*H*-indol-4-ol with 2-(2-hydroxyethyl)isindoline-1,3-dione (II 25 and II 26). The following Boc-deprotection or methylaminolysis provided the desired amines. For a detailed description of the synthetic procedures used in the synthesis on amines, see the Supporting Information.

The final reaction of reductive amination was carried out in the presence of 1,4-diazabicyclo[2.2.2]octane (DABCO) as a base, sodium cyanoborohydride (NaCNBH₃) as a reducing agent, and with addition of iron sulfate heptahydrate (FeSO₄ × 7H₂O) that complexes cyanide ions and therefore contributes to the improvement of the reaction yields. In an additional step, indole derivative 56 was reduced to indoline analogue 57.

Structure-Affinity Relationships. 5-HT_{1A} Receptor Affinity. All the obtained compounds were subjected to affinity determination using radioligand binding studies. The affinity of

Scheme 1. Synthesis of 1-(1-Benzoyl-4-fluoropiperidin-4-yl)methanamine Derivatives^a

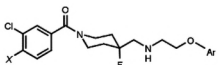
^aReagents and conditions: (i) DABCO, NaCNBH₃, FeSO₄ × 7H₂O, molecular sieves, MeOH, r.t., 36–72 h, yield: 18–82%; (ii) 1.0 M HCl in EtOAc, r.t., 24 h, yield: 48%; (iii) CH₃COOH, NaCNBH₃, 15 °C—15 min, then r.t.—1 h, yield: 67%. X = F or Cl.

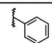
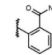
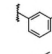
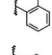
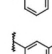
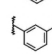
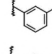
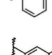
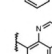
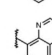
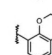
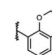
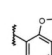
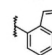
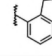
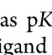
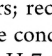
Scheme 2. Synthesis of the Amine Intermediates (6–26)^a

^aReagents and conditions: (i) for compounds II 24–26, *tert*-butyl-2-hydroxyethyl carbamate or 2-(2-hydroxyethyl)isoindoline-1,3-dione, PPh₃, DIAD, THF, 0 °C then r.t., 24 h, and 50 °C, 24 h; (ii) 1,2-dibromoethane, K₂CO₃, acetone, 40–80 °C, 24–72 h; (iii) for compounds II 6–16, 18–23, potassium phthalimide, 18-crown-6 ether, DMF, 50 °C, 3 h; (iv) NaH, CH₃I, THF, 0 °C, 30 min, then r.t., 1 h; for compound II 17 (iv) and then (iii); (v) for compounds 6–23, 25, 26, 40% MeNH_{2(aq)}, 10% NaOH, 50 °C, 2 h, then r.t., 1 h. (vi) For compound 24, 1.0 M HCl in EtOAc, r.t., 24 h; R1 = phthalimide or *tert*-butyl carbamate.

the compounds at 5-HT_{1A} receptors was generally high, with pK_i values ranging from 8.18 to 12.80 (Tables 1 and 2). To determine the influence of various phenyl ring substitutions on affinity and exclude the contribution of lipophilicity, we primarily focused on analyzing changes of ligand-lipophilicity efficiency (LLE), calculated as the difference between pK_i and ClogD_{7.4}. All the relationships were compared to the unsubstituted phenoxy derivative 3 (LLE 7.59), which was the lead structure for this series (Figure 5).

First, we focused on checking the effect of the substitution site on the phenyl ring using three commonly used substituents (F, Cl, or OCH₃). The substitution in the *ortho* position increased the binding affinity; however, the effect was rather modest and did not exceed 0.5 LLE units. The effect of substitution in the *meta* position was diversified, ranging from slight increase of affinity for fluoro and methoxy analogues to decrease in the case of the chloro derivative. On the other hand, substitution in the *para* position generally decreased the affinity by up to 2 LLE units. The negative effect of a *para*

Table 2. Influence of the Type of Substituent in the Phenyl Ring on 5-HT_{1A} Receptor Affinity and Selectivity for the Most Important Off-Targets


Compd	X	Ar	receptor affinity ^a (pK _i)				
			5-HT _{1A} ^{b,e}	α ₁ ^{c,f}	D ₂ ^{d,g}	ClogD _{7.4} ^h	LLE ⁱ
3	F		10.21 ± 0.20	6.29 ± 0.13	< 6.00	2.62	7.59
42	F		10.22 ± 0.21	< 6.00	< 6.00	1.51	8.71
43	F		10.53 ± 0.24	< 6.00	< 6.00	1.49	9.05
44	F		9.93 ± 0.22	6.04 ± 0.01	< 6.00	2.08	7.86
45	F		10.47 ± 0.19	< 6.00	< 6.00	2.09	8.38
46	F		9.52 ± 0.15	< 6.00	< 6.00	2.72	6.79
47	F		10.08 ± 0.13	< 6.00	< 6.00	1.86	8.21
48	Cl		10.27 ± 0.21	< 6.00	< 6.00	2.33	7.95
49	F		9.85 ± 0.23	< 6.00	< 6.00	3.13	6.72
50	F		9.56 ± 0.02	< 6.00	< 6.00	3.51	6.05
51	F		10.22 ± 0.25	6.76 ± 0.03*	< 6.00	2.82	7.40
52	Cl		9.37 ± 0.03	6.69 ± 0.07	6.36 ± 0.14	3.28	6.09
53	F		9.86 ± 0.11	6.72 ± 0.13*	< 6.00	2.17	7.69
54	Cl		9.71 ± 0.12	6.71 ± 0.02*	6.04 ± 0.12	2.63	7.08
55	F		11.07 ± 0.06	7.76 ± 0.32*	7.54 ± 0.12*	3.22	7.85
56	F		12.80 ± 0.16	7.00 ± 0.05	< 6.00	2.74	10.06
57	F		10.35 ± 0.02	6.36 ± 0.02	< 6.00	2.12	8.23

^aAll binding affinity values are represented as pK_i (i.e., -logK_i) and expressed as means ± SEM from at least three experiments performed in duplicate, unless otherwise indicated; radioligand binding was performed using ^bCHO-K1 cells transfected with 5-HT_{1A} receptors. ^cRat cortex. ^dCHO-K1 cells transfected with D₂ receptors; receptor affinity values were determined by competition binding using ^e[³H]8-OH-DPAT. ^f[³H]-prazosin and ^g[³H]-methylspiperone. In these conditions, pK_i of phentolamine at α₁ receptors was 7.95, and pK_i of haloperidol at D₂ receptors was 8.85. ^hCalculated distribution coefficient at pH 7.4. ⁱLLE referring to the 5-HT_{1A} receptor. * pK_i value was expressed as mean ± range from two experiments performed in duplicate.

subnanomolar or even picomolar K_i values and generally very high LLE values.

The most pronounced increase in 5-HT_{1A} receptor affinity was noted in the case of derivatives containing H-bond donor (HBD) moiety at the meta position (45, 47, 56, and 57). Worth mentioning is the fact that one of the meta-HBD derivatives, compound 56, had an exceptionally high affinity, reaching subpicomolar values (pK_i 12.80, K_i 0.16 pM, LLE 10.06). The increase in binding affinity of the derivatives with HBD in the meta position can be explained by their ability to create an additional hydrogen bond with serine Ser5.42 in the binding site of the 5-HT_{1A} receptor (Figure 4). This stabilizes the ligand–receptor complex and lowers the binding energy (IFD score for compound 56 = -465.26 compared to -463.69 for compound 3).

The hypothesis that creating a hydrogen bond in this region improves binding affinity was further supported by the marked increase in LLE for the benzamide derivatives (42 and 43), which are also capable of forming this interaction. Moreover, the meta derivatives not capable of forming H-bonds (46, 49, 50) displayed lower affinity, which is consistent with the observation made for compound 33 (a meta-chloro derivative) and suggests that they exert a negative steric contribution (this was, however, less pronounced than in the case of the para analogues).

Regarding the substitution at the benzoyl moiety, the 4-chloro analogues had overall lower LLE than their 4-fluoro counterparts, suggesting that this modification is not generally favorable.

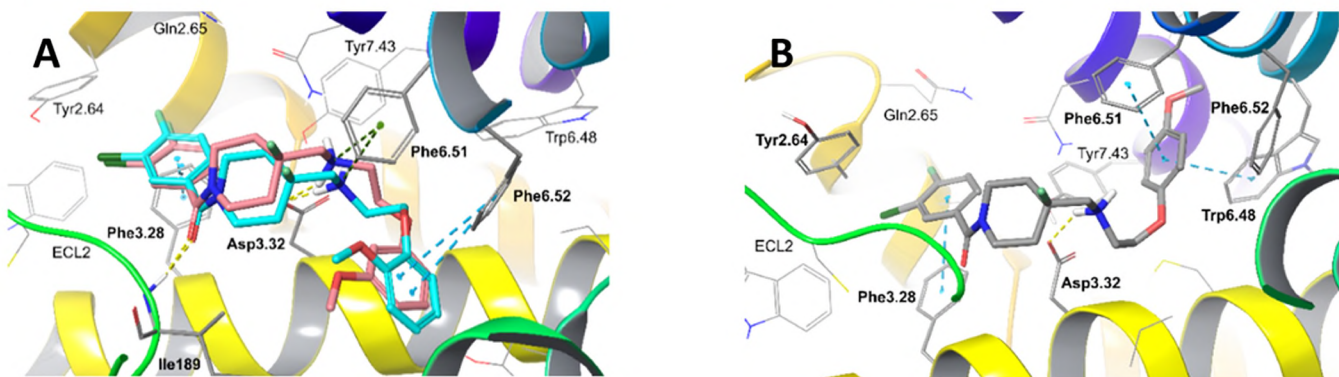


Figure 2. Predicted binding mode of the methoxy derivatives, that is, compound 36 (light teal) together with 38 (pink) (A) and compound 40 (gray) (B) in the site of the serotonin 5-HT_{1A} receptor. Amino acid residues engaged in ligand binding (within 4 Å from the ligand atoms) are displayed as sticks, whereas crucial residues, for example, forming H-bonds (dotted yellow lines), π - π /CH- π stacking (dotted cyan lines), and cation- π interactions (dotted green line) are represented as thick sticks. ECL2 residues were hidden for clarity; ECL—extracellular loop. The homology model of the 5-HT_{1A} receptor is based on the crystal structure of the 5-HT_{1B} receptor (PDB ID: 4IAR).

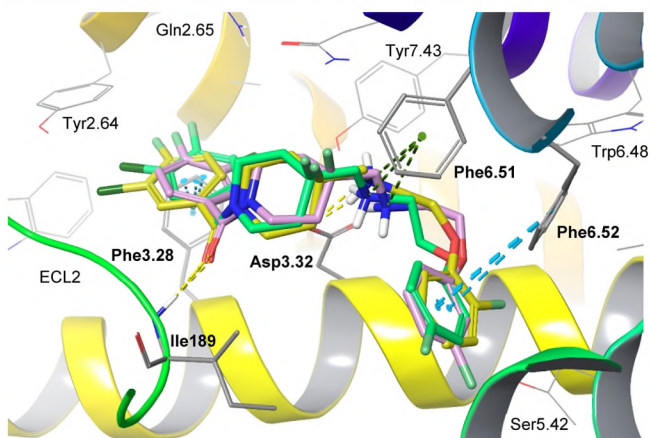


Figure 3. Predicted binding mode of the fluoro derivatives, that is, compound 28 (yellow) together with 29 (pink) and 31 (green) in the site of the serotonin 5-HT_{1A} receptor. Amino acid residues engaged in ligand binding (within 4 Å from the ligand atoms) are displayed as sticks, whereas crucial residues, for example, forming H-bonds (dotted yellow lines), π - π /CH- π stacking (dotted cyan lines), and cation- π interactions (dotted green line) are represented as thick sticks. ECL2 residues were hidden for clarity; ECL—extracellular loop. The homology model of the 5-HT_{1A} receptor is based on the crystal structure of the 5-HT_{1B} receptor (PDB ID: 4IAR).

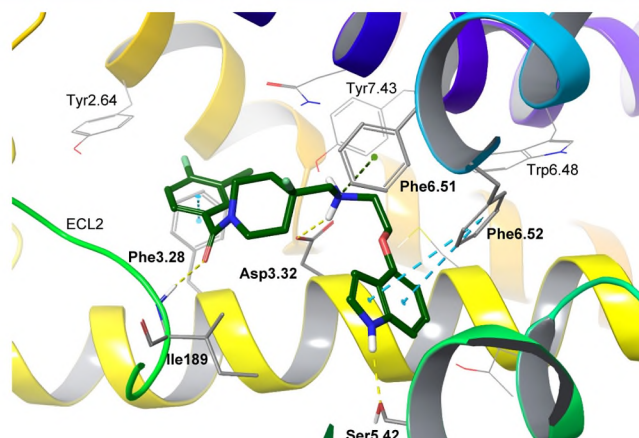


Figure 4. Predicted binding mode of compound 56 (with HBD in meta position) in the site of the serotonin 5-HT_{1A} receptor. Amino acid residues engaged in ligand binding (within 4 Å from the ligand atoms) are displayed as sticks, whereas crucial residues, for example, forming H-bonds (dotted yellow lines), π - π /CH- π stacking (dotted cyan lines), and cation- π interactions (dotted green line) are represented as thick sticks. ECL2 residues were hidden for clarity; ECL—extracellular loop. The homology model of the 5-HT_{1A} receptor is based on the crystal structure of the 5-HT_{1B} receptor (PDB ID: 4IAR).

Selectivity versus Key Antitargets, the Adrenergic α_1 and Dopaminergic D₂ Receptors. Previous studies of 1-(1-benzoylpiperidin-4-yl)methanamine derivatives indicated that the highest risk of off-target interactions is with adrenergic α_1 and dopaminergic D₂ receptors.^{13,27–29} Accordingly, all the novel compounds were tested for binding to these receptors to confirm their selectivity (Tables 1 and 2).

Concerning α_1 receptor affinity, the majority of the compounds showed very high selectivity for 5-HT_{1A} over α_1 and D₂ receptors (over 1000–10,000 times). In general, increased affinity for the α_1 receptor was observed for the *ortho*-substituted analogues (36, 37, 44). The highest affinities (pK_i 6.6–7.8) were observed for the derivatives with the *ortho*-methoxy substituent (36, 37) and their bicyclic analogues, with oxygen or nitrogen in the *ortho* position (51, 52, 53, 54, 55). High α_1 receptor affinity was also observed for the indole derivative 56 (pK_i 7.00). Interestingly, the *ortho*-fluoro- and *ortho*-chloro-derivatives (28, 32) did not show significant

affinity for the α_1 receptor ($pK_i < 6$), indicating that halogen in this position impairs α_1 receptor binding. In comparison, literature data indicate that *ortho*-methoxy- or *ortho*-ethoxy-substitution in the aryl moiety increase α_1 receptor affinity. For example, in the structure of tamsulosin, a selective α_{1A} receptor antagonist used for the treatment of benign prostatic hyperplasia, a 2-(2-ethoxyphenoxy)ethanamine fragment, can be highlighted.³⁰ Nevertheless, it should be noted that selectivity for 5-HT_{1A} versus α_1 receptors was generally very high and was less than 1000 \times for only two compounds (37, 52).

In the case of the D₂ receptor, only one compound (55) showed substantial affinity (pK_i D₂ 7.54). This observation is in line with the fact that the 2,2-dimethyl-2,3-dihydro-1-benzofuran moiety was previously used in the structure of dual acting, 5-HT_{1A}R agonist/D₂R antagonist ligands.³¹ However, the affinity of 55 for the D₂ receptor did not significantly affect selectivity because its affinity for the 5-HT_{1A} receptor was still

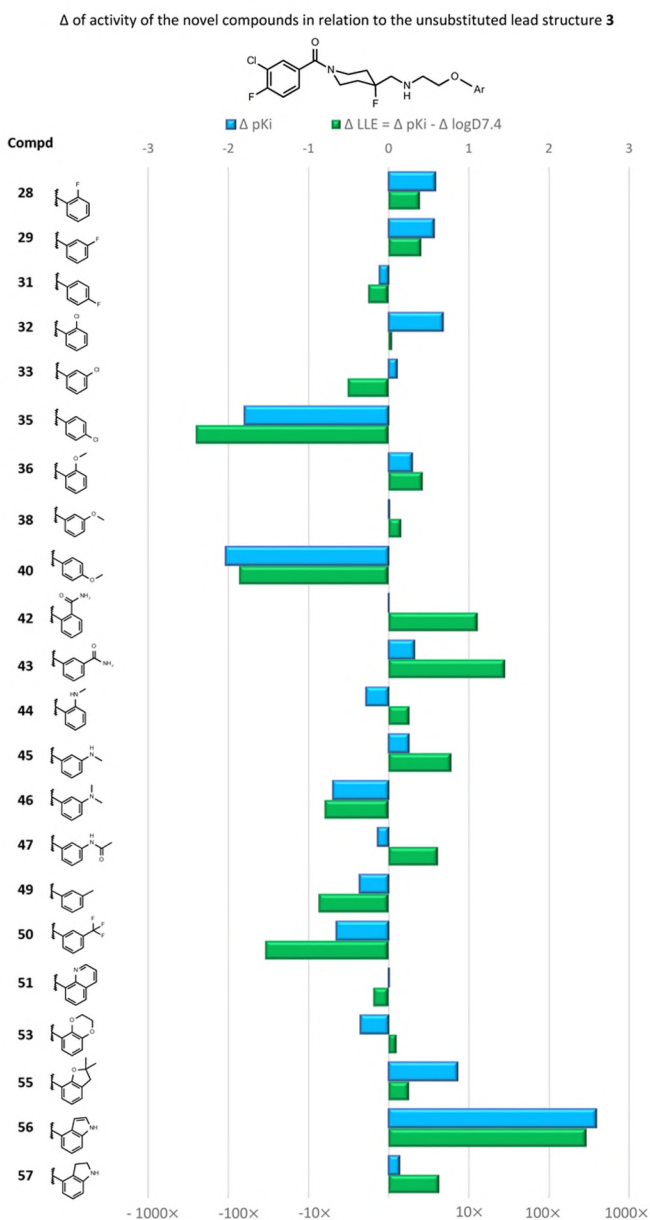


Figure 5. Changes in LLE in relation to unsubstituted lead structure 3 due to substitution at the phenyl ring.

over 3.5 orders of magnitude higher ($>3000\times$, pK_i 5-HT_{1A} = 11.07).

Summing up, most of the presented compounds showed substantial selectivity versus key antitargets (K_i ratio over 1000-fold) although the phenoxyethanamine scaffold is common also for ligands of other monoaminergic receptors. This supports the finding that the 1-[4-(aminomethyl)-4-fluoropiperidin-1-yl]ethan-1-one core is the essential scaffold for providing both high affinity and high selectivity for the 5-HT_{1A} receptor.

Structure-Functional Activity Relationships. Based on the results of the studies described above, 25 compounds were selected for functional studies. The functional profiles of the novel compounds were measured at several pathways engaged in 5-HT_{1A} receptor signal transduction. Compounds were tested in four functional assays: ERK1/2 phosphorylation (pERK1/2), adenylyl cyclase inhibition (cAMP), β -arrestin recruitment (β -arrestin), and calcium mobilization (Ca^{2+}). To

classify the agonist efficacy of the compounds, we assumed that E_{max} values higher than 80% relative to the maximal effect of serotonin are characteristic of a full agonist, between 79 and 21% of a partial agonist, and 20% or less, indicating negligible agonist activity. The experiments were carried out using cell lines expressing the recombinant human 5-HT_{1A} receptor.

In terms of potency, the general trends (Tables 3 and 4) were similar to those established in affinity studies. Compared to 3, the derivatives substituted with the HBD in the meta position (43, 45, 47, 48) were characterized by a rise in potency in all the signaling pathways. The same trend was observed for the bicyclic analogues (51, 55, 56, 57), but the other derivatives showed mostly decreased potency in functional assays. The notable exceptions were compound 36 and 38, the *ortho*- and *meta*-methoxy analogues, respectively, which were characterized by generally higher potency than 3 as well as compound 42, an *ortho*-carboxamido analogue, which displayed potency similar to 3, with modest variations in both sides. The extent of potency change varied between individual analogues in terms of signaling pathways, resulting in diversified functional selectivity profiles for some of them.

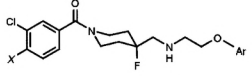
The efficacy of the ligands for the ERK1/2, cAMP, and β -arrestin pathways was generally high, falling slightly below 80% in only a few cases. The vast majority of the compounds can therefore be considered as full agonists in those signaling pathways. On the other hand, most of the compounds showed lower efficacies in the calcium mobilization assay. Thirteen compounds were classified as partial agonists and two even as negligibly active, as they showed marginal level of stimulation (15%). Both these compounds were para-substituted analogues (35 and 40).

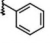
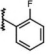
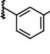
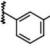
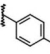
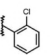
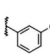
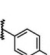
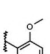
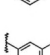
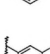
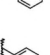
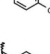
Bias Factors. The functional selectivity of the ligands was analyzed by calculating bias factors. These compare the efficacy and potency of compounds for pairs of signaling pathways using the following equation^{32–35}

$$\begin{aligned} \text{bias factor} &= \log \left(\frac{\text{relative activity}_{12,\text{lig}}}{\text{relative activity}_{12,\text{ref}}} \right) \\ &= \log \left(\frac{\left(\frac{E_{\max,\text{path1}} \times EC_{50,\text{path2}}}{EC_{50,\text{path1}} \times E_{\max,\text{path2}}} \right)_{\text{lig}}}{\left(\frac{E_{\max,\text{path1}} \times EC_{50,\text{path2}}}{EC_{50,\text{path1}} \times E_{\max,\text{path2}}} \right)_{\text{ref}}} \right) \end{aligned}$$

The calculations in the present study follow the same approach as in our previous study.¹³ Briefly, the bias factor provides a measure that integrates E_{max} and EC_{50} values of both a test ligand and a reference compound (*i.e.* serotonin). Results are presented in Tables 5 and 6 and compounds which displayed that a significant bias (over 1 log) was highlighted in green (for positive values) or in blue (for negative values). Those compounds which showed significant bias, but with low pEC_{50} values, were marked in gray.

ERK1/2 versus cAMP. Most of the compounds showed a preference for ERK1/2 phosphorylation, with the highest bias factors (>1 log) being found for compounds 40, 44, and 55. The highest ERK1/2 phosphorylation preference was found for compound 55 with a bias factor of 2.8 log. Three compounds (47, 48, and 51), preferred the cAMP pathway

Table 3. Functional Activity of Compounds 28–33, 35, 36, 38–41 at 5-HT_{1A} Receptors


Compd	X	Ar	5-HT _{1A} functional activity ^a							
			ERK1/2 ^b		cAMP ^b		β-arrestin ^c		Ca ²⁺ ^b	
			E _{MAX}	pEC ₅₀	E _{MAX}	pEC ₅₀	E _{MAX}	pEC ₅₀	E _{MAX}	pEC ₅₀
3	F		92%	9.10	90%	8.09	96%	7.98	91%	7.20
28	F		95%	8.24	89%	7.74	97%	7.61*	90%	6.82*
29	F		96%	8.64	99%	7.80	91%	7.46	73%	7.16*
30	Cl		93%	7.70	89%	7.40	104%	6.21*	90%	6.19*
31	F		98%	8.24	96%	7.37	99%	7.06*	73%	7.00
32	F		NT ^d	NT ^d	87%	7.59	94%	7.76	36%	6.26*
33	F		97%	7.99	88%	7.71	99%	6.65*	80%	6.60*
35	F		88%	6.93	63%	6.32	109%	6.01*	15%	5.28
36	F		NT ^d	NT ^d	83%	9.86*	90%	9.43	54%	9.52*
38	F		97%	9.40	89%	8.98	90%	8.64*	64%	7.15
39	Cl		95%	8.14	96%	7.69	95%	6.91	74%	6.50
40	F		86%	7.68	88%	6.25	82%	5.79	15%	6.21
41	Cl		78%	7.32	59%	6.48	65%	5.60	24%	5.88*
1			100%	8.33	92%	7.22	98%	6.71	66%	6.52
(±) 8-OH-DPAT			93%	8.09	63%	7.50	101%	7.84	35%	7.66
Buspirone			44%	7.82	49%	7.14	100%	6.73	8.3%	7.42*
Serotonin ^e			100%	7.48	100%	7.51	100%	6.89	100%	7.23

^aAll the functional activity values were expressed as means from at least three experiments performed in duplicate, unless otherwise indicated. For the sake of clarity, the SEM values were omitted in this table and are presented in the Supporting Information—Table S1; the functional assay was performed using ^bCHO-K1 cells. ^cU2OS cells (Tango LiveBLazer assay kit). ^dNT—not tested; * value was expressed as mean from two experiments performed in duplicate. ^eData for Serotonin on ERK, cAMP, and β-arrestin are reproduced from the previous paper.¹³

and significant bias was observed for compound 47 (bias factor −1.03).

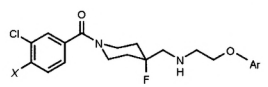
When comparing 3-chloro-4-fluorobenzoyl derivatives (29, 38, 40, 47) with their 3,4-dichlorobenzoyl derivative counterparts (30, 39, 41, 48), it is noticeable that the former always show a more pronounced biased profile than the latter compounds.

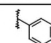
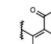
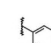
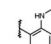
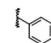
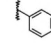
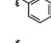
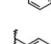
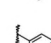
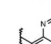
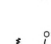
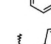
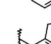

ERK1/2 versus β-Arrestin. Three compounds preferred ERK1/2 phosphorylation versus β-arrestin, and four compounds preferred β-arrestin recruitment versus ERK1/2 phosphorylation. This is the first time, to our knowledge, that β-arrestin-biased agonists have been reported for the selective 5-HT_{1A} receptor ligands. Bias factors for the ERK1/2-biased agonists ranged from 1.21 for compound 41 to 1.43 for

compound 44, whereas in the case of β-arrestin-biased agonists, their bias factors were much more pronounced (from −1.95 for 48 to −3.71 log for 56).

The ERK1/2-preferring compounds were the *para*-methoxy derivatives (40 and 41) and the *ortho*-methylamine derivative 44. On the other hand, the compounds that showed bias for β-arrestin recruitment were either the bicyclic aromatic derivatives (51 and 56) or *meta*-acetamido derivatives (47 and 48).

It is noticeable that the *ortho*-methylamine-substituted derivative (44) showed substantial ERK1/2 bias (1.43), while the *meta*-methylamine-substituted derivative (45) showed an opposite preference (bias factor −0.60).

Table 4. Functional Activity of Compounds 42–51 and 55–57 at 5-HT_{1A} Receptors


Compd	X	Ar	5-HT _{1A} functional activity ^a							
			ERK1/2 ^b		cAMP ^b		β-arrestin ^c		Ca ²⁺ ^b	
			E _{MAX}	pEC ₅₀	E _{MAX}	pEC ₅₀	E _{MAX}	pEC ₅₀	E _{MAX}	pEC ₅₀
3	F		92%	9.10	90%	8.09	96%	7.98	91%	7.20
42	F		92%	8.68	95%	8.22	101%	8.08*	84%	7.53
43	F		87%	9.74	92%	9.18	101%	8.55	105%	7.42*
44	F		89%	8.86	77%	7.82	96%	6.79	43%	6.99*
45	F		83%	10.13	87%	9.95	100%	10.05	94%	7.49
46	F		87%	8.22	91%	7.77	101%	7.22	82%	6.86*
47	F		102%	9.75	89%	10.86*	93%	12.68	100%	7.66*
48	Cl		100%	9.23	94%	10.18	96%	10.60*	100%	7.36*
49	F		93%	8.72	82%	7.83	98%	7.27*	59%	6.83
50	F		100%	7.25	99%	6.56	104%	6.14*	73%	6.14
51	F		96%	9.30	104%	9.47	92%	11.83*	67%	7.87
55	F		81%	10.99	88%	8.18	99%	9.49	89%	7.27*
56	F		102%	10.53	96%	10.06	94%	13.67	79%	7.84
57	F		94%	11.44	89%	10.88	92%	11.29	56%	8.45*

^aAll the functional activity values were expressed as means from at least three experiments performed in duplicate, unless otherwise indicated. For the sake of clarity, the SEM values were omitted in this table and are presented in the Supporting Information—Table S1; the functional assay was performed using ^bCHO-K1 cells. ^cU2OS cells (Tango LiveBLazer assay kit); * value was expressed as mean from two experiments performed in duplicate.

ERK1/2 versus Ca²⁺. In general, most of the compounds showed substantial bias for ERK1/2 phosphorylation versus calcium mobilization (Ca²⁺) and none of the tested compounds showed preference for Ca²⁺. The highest ERK1/2 preference was found for the benzo-fused, five-membered ring derivatives (55–57), reaching a bias factor of 3.42 for compound 55.

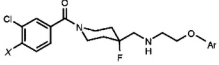
cAMP versus β-Arrestin. Only five compounds (30, 33, 39, 41, 44) exhibited some preference toward cAMP inhibition, however not exceeding half a log, whereas the rest of the compounds preferred β-arrestin recruitment. As seen for ERK1/2 versus cAMP bias, a favorable influence of the 3,4-dichlorobenzoyl moiety on cAMP potency was observed here, as compared to the corresponding 3-chloro-4-fluorobenzoyl analogues.

Among the derivatives with marked β-arrestin recruitment bias, compounds 47, 48, 51, and 56 were identified again, as in the case of preference for β-arrestin versus ERK1/2. Interestingly, compound 55 also preferred β-arrestin pathway versus cAMP, although previously it exhibited the highest preference for ERK1/2 versus β-arrestin. This is due to its very

high potency in the ERK1/2 assay (pEC₅₀ 10.99) and also relatively high β-arrestin potency (pEC₅₀ 9.49), as compared to other assays, where its potency was noticeably weaker.

Overall, it should be noted that preference toward β-arrestin recruitment was much higher than for the most biased reference compound, (±) 8-OH-DPAT (−1.18), and reached an extremely high value (−4.24) for compound 56.

Previous studies by Stroth and co-workers are worth mentioning, where the authors identified 5-HT_{1A}-biased ligands with a strong preference for cAMP over β-arrestin signaling.³⁶ However, it should be noted that those arylpiperazine derivatives had only partial agonist properties in the cAMP assay (53–73%). They also showed very low E_{max} values in the β-arrestin assay (6–36%). Noteworthy, Stroth *et al.* reported that the reference agonist (±) 8-OH-DPAT achieved only 44% efficacy in the β-arrestin assay, while herein it reached 101%, so the observed differences in signaling bias may be at least partially due to the methodological differences (β-arrestin assay in that study was performed using Path-Hunter eXpress HTR1A CHO-K1 β-Arrestin GPCR Assay

Table 5. Bias Factors of Compounds (28–33, 35, 36, 38–41) and References at 5-HT_{1A} Receptors


Compd	X	Ar	5-HT _{1A} receptor bias factor (logarithmic value)					
			ERK1/2 vs. cAMP	ERK1/2 vs. β-arrestin	ERK1/2 vs. Ca ²⁺	cAMP vs. β-arrestin	cAMP vs. Ca ²⁺	β-arrestin vs. Ca ²⁺
3	F		1.05	0.51	1.65	-0.54	0.60	1.15
28	F		0.56	0.03	1.19	-0.53	0.63	1.16
29	F		0.85	0.60	1.35	-0.25	0.50	0.75
30	Cl		0.35	0.85	1.27	0.50	0.92	0.42
31	F		0.90	0.57	1.11	-0.33	0.20	0.54
32	F		– ^a	– ^a	– ^a	-0.83	1.42	2.25
33	F		0.35	0.73	1.22	0.38	0.86	0.48
35	F		0.78	0.23	2.15	-0.55	1.38	1.92
36	F		– ^a	– ^a	– ^a	-0.23	0.24	0.47
38	F		0.49	0.19	2.17	-0.30	1.68	1.98
39	Cl		0.48	0.63	1.49	0.15	1.02	0.87
40	F		1.44	1.31	1.98	-0.13	0.54	0.67
41	Cl		1.00	1.21	1.70	0.21	0.70	0.49
1			1.17	1.02	1.76	-0.15	0.59	0.74
(±) 8-OH-DPAT			0.79	-0.39	0.59	-1.18	-0.20	0.98
Buspirone			0.66	0.14	0.86	-0.52	0.21	0.73
5-HT			0.00	0.00	0.00	0.00	0.00	0.00

^aNo data for pERK assay. Compounds that displayed a significant bias (over 1 log) are highlighted in green (for positive values) or in blue (for negative values). Those compounds that showed significant bias but with low pEC₅₀ values are marked in gray.

DiscoverRx and in the current study using Tango HTR1A-bla U2OS LiveBLazer assay kit, Life Technologies).

cAMP versus Ca²⁺. Eleven compounds markedly preferred the cAMP pathway versus Ca²⁺. Noteworthy, the most biased compounds (with bias factors over 2) had HBD in the meta position (45, 47, 48, 56, and 57), further indicating the positive influence of this substituent on cAMP inhibition potency. Because of relatively low potency of all the compounds in the calcium mobilization assay, none of them exhibited bias toward this signaling pathway.

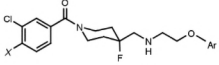
β-Arrestin versus Ca²⁺. Thirteen compounds were markedly biased for β-arrestin. Four of the compounds (47, 48, 51, and 56) showed extremely high bias for β-arrestin (over 3.5 log), reaching a 6.25 log value (over 1,000,000 times) for compound 56. The relatively lower ability of the compounds to stimulate Ca²⁺ mobilization resulted in a lack of noticeable Ca²⁺-preferring biases.

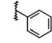
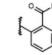
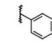
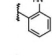
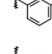
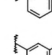
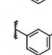
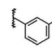
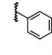
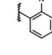
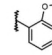
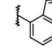
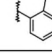
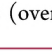
“Signaling Fingerprint” Analysis. The functional studies enabled selection of biased agonists that exhibit preference for specific pathways. To describe the pattern of behavior of the compounds in the different pathways, we calculated “signaling

fingerprints” based on measures of potency and efficacy and represented them as bars of particular height and color intensity (heat map), respectively. The potency of each ligand in a particular assay was normalized according to the performance of the native neurotransmitter (*i.e.*, serotonin) in this assay. It was calculated using the following equation:

$$\text{normalized ligand potency} = -\log \left(\text{EC}_{50 \text{ path}_{\text{lig}}} \div \left(\frac{\text{EC}_{50 \text{ path}}}{\text{EC}_{50 \text{ ref. path}}^{\text{native ligand}}} \right) \right)$$

A “signaling fingerprint” therefore allows for the simultaneous comparison of a ligand’s functional profile in all pathways. “Signaling fingerprints” were calculated for both the reference and the novel compounds, including all four tested pathways, with serotonin as the native ligand and cAMP as the reference pathway (due to a relatively higher potency of serotonin in this assay). Significant preference of a given

Table 6. Bias Factors of Compounds 42–51 and 55–57 at 5-HT_{1A} Receptors


Compd	X	Ar	5-HT _{1A} receptor bias factor (logarithmic value)					
			ERK1/2 vs. cAMP	ERK1/2 vs. β -arrestin	ERK1/2 vs. Ca ²⁺	cAMP vs. β -arrestin	cAMP vs. Ca ²⁺	β -arrestin vs. Ca ²⁺
3	F		1.05	0.51	1.65	-0.54	0.60	1.15
42	F		0.47	-0.04	0.93	-0.51	0.46	0.97
43	F		0.57	0.53	1.98	-0.04	1.42	1.45
44	F		1.13	1.43	1.93	0.31	0.81	0.50
45	F		0.20	-0.60	2.33	-0.80	2.14	2.93
46	F		0.45	0.33	1.12	-0.12	0.67	0.79
47	F		-1.03	-3.49	1.85	-2.47	2.87	5.34
48	Cl		-0.90	-1.95	1.61	-1.06	2.50	3.56
49	F		0.97	0.83	1.84	-0.14	0.87	1.01
50	F		0.73	0.49	1.00	-0.23	0.27	0.50
51	F		-0.17	-3.11	1.33	-2.94	1.50	4.44
55	F		2.80	0.81	3.42	-1.99	0.62	2.61
56	F		0.53	-3.71	2.54	-4.24	2.02	6.25
57	F		0.61	-0.44	2.95	-0.99	2.34	3.39

Compounds that displayed a significant bias (over 1 log) are highlighted in green (for positive values) or in blue (for negative values).

pathway was defined in this study as a difference in normalized ligand potency of at least 1 order of magnitude (1 log).

Among the reference compounds (Figure 6), the most biased was compound 1, showing significant preference for ERK1/2 phosphorylation over all other assays, which is in line with previous studies.^{12,13} On the other hand, (\pm) 8-OH-DPAT displayed a 1 log preference for the β -arrestin versus cAMP pathway but was unbiased with respect to other pathways. Buspirone, consistent with its partial agonist properties, showed low efficacy in all assays but β -arrestin, which was particularly evident for calcium mobilization (E_{\max} 8.3%); the potencies, however, did not differ significantly.

The “signaling fingerprints” for the most interesting novel compounds, in comparison with the lead structures 2 and 3, are shown in Figure 7. In the rows, the analogues with structurally closest substituents were collected to show the gradual impact of their modification on changes in the functional profile. The pERK1/2-preferring analogues are shown in the left column, the more balanced in the middle, and the β -arrestin-biased agonists in the right column.

Based on the more detailed analysis of the “signaling fingerprints”, the novel 5-HT_{1A} receptor agonists can be categorized into three types, divided into five subtypes, each with a different functional selectivity profile. Type I includes ligands with a significant preference for ERK1/2 phosphor-

ylation and a diverse profile of activity in other assays, which is mainly differentiated by the level of activation of β -arrestin recruitment. Type IA, including compounds 44 and 2, consists of ligands which showed significant preference for ERK1/2 phosphorylation over all other pathways, similar to the reference biased agonist, 1. Compounds 3 and 55, which were classified into type IB, were characterized by a significant preference for ERK1/2 phosphorylation over cAMP and Ca²⁺, but not β -arrestin. Type II includes compounds 45 and 57, which show a similar level of activity in ERK1/2, cAMP, and β -arrestin assays, with a slight preference for the latter.

In contrast to types I and II, and of particular interest in the present study, are type III compounds: these include first-in-class ligands that strongly prefer β -arrestin recruitment over all other signaling pathways. It is noteworthy that such a profile was not observed for any of the reference compounds, and, to our knowledge, has not been previously described in the literature, which could imply that these compounds may exhibit novel pharmacological and, potentially, therapeutic properties. Type IIIA (compounds 51 and 56) includes ligands characterized by the strongest preference of the β -arrestin pathway, similar levels of activity in ERK1/2 and cAMP assays, and much lower stimulation of Ca²⁺. Type IIIB, represented by compound 47, is characterized by the high levels of activity in both β -arrestin and cAMP assays (with especially marked

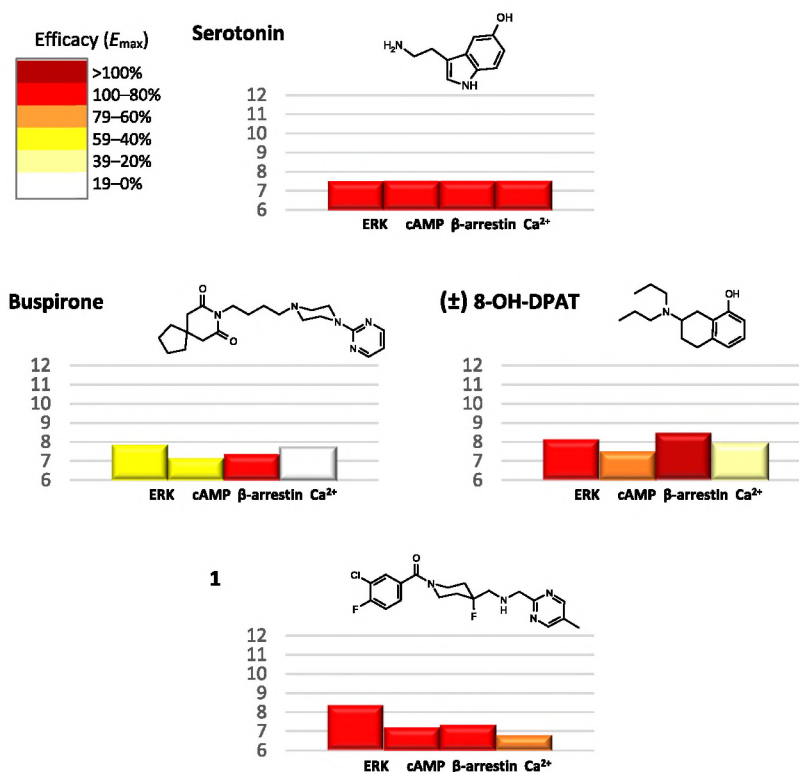


Figure 6. “Signaling fingerprints” for reference compounds (bar height—normalized ligand potency in log scale, bar color—ligand efficacy, as percent E_{max}).

activity of β -arrestin pathway) and lower ability to activate ERK1/2 phosphorylation and calcium mobilization. Noteworthy, compound 47 was the only one that showed significant preference for activity (above 1 log) in the cAMP assay over ERK1/2 phosphorylation.

Summing up, the following structure functional selectivity relationships could be inferred:

- (1) the presence of an H-bond-forming substituent in the *ortho* position of the phenoxyethyl moiety (44, 55) or a nitrogen atom built in the aryl ring in the same position (2) decreases the ability to activate β -arrestin recruitment in the tested group of 5-HT_{1A} receptor agonists, thus relatively enhancing a preference for ERK1/2 phosphorylation.
- (2) substitution of the HBD moiety in the meta position of the phenoxyethyl moiety (45, 57) increases agonist potency in all signaling pathways, with the effect being especially pronounced for cAMP inhibition and β -arrestin recruitment. Except for calcium mobilization being substantially weaker, those potent agonists do not distinguish significantly between other pathways.
- (3) in contrast, the derivatives with a bicyclic aromatic moiety (56 and 51) or a flat, π -electron-containing substituent (e.g. 47) exhibited particular preference for β -arrestin recruitment, yielding very strong activity in this assay. Noteworthy, replacement of an aromatic indole moiety of 56 with a partially saturated indoline (57) markedly decreased β -arrestin recruitment, resulting in no particular preference over ERK1/2 phosphorylation or cAMP inhibition, thus confirming this finding. It should be noted that, to our knowledge, these compounds are the first 5-HT_{1A} ligands to show such a strong biased agonism for β -arrestin recruitment and

this, in itself, constitutes an intriguing novel finding in drug discovery at this receptor.

More broadly, these *in vitro* data strongly indicate that it is possible to identify specific structural motifs that are responsible for directing 5-HT_{1A} receptor signaling to distinct intracellular responses.

Developability Studies. The developability of the novel compounds was initially assessed *in silico* using LELP, Fsp3, and CNS-MPO measures (Table S2). Majority of the compounds showed favorable score values, thus testifying to the overall promising developability potential of the explored series. In order to support the choice of proper candidates for *in vivo* tests, selected *in vitro* developability studies were performed. As a first step, the novel compounds displaying the most interesting functional profiles were tested for preliminary metabolic stability using RLMs (Table S3). The stability was assessed referring to the marketed drugs of different stabilities, aripiprazole and verapamil, showing high or low stability in the given conditions, respectively. Various levels of stability were found for the novel compounds, ranging from high stability for compounds 47, 48, 51, and 56 (73–87%), through medium stability for compounds 2, 3, and 44 (54–59%), to low stability for compounds 55 and 57 (21 and 37%). Based on the functional studies and the above results, compound 56, a β -arrestin recruitment-biased agonist with high metabolic stability, and compound 44, an ERK1/2 phosphorylation-prefering ligand with medium metabolic stability, were selected for further studies. To confirm preliminary metabolic stability data, for the lead structure 3 as well as compounds 44 and 56, intrinsic clearance was determined in comparison with the reference CNS drugs aripiprazole and diazepam (Table 7). As expected, compound 44 and the lead structure 3 showed the same level of medium metabolic stability (CL_{int} 48.8 and

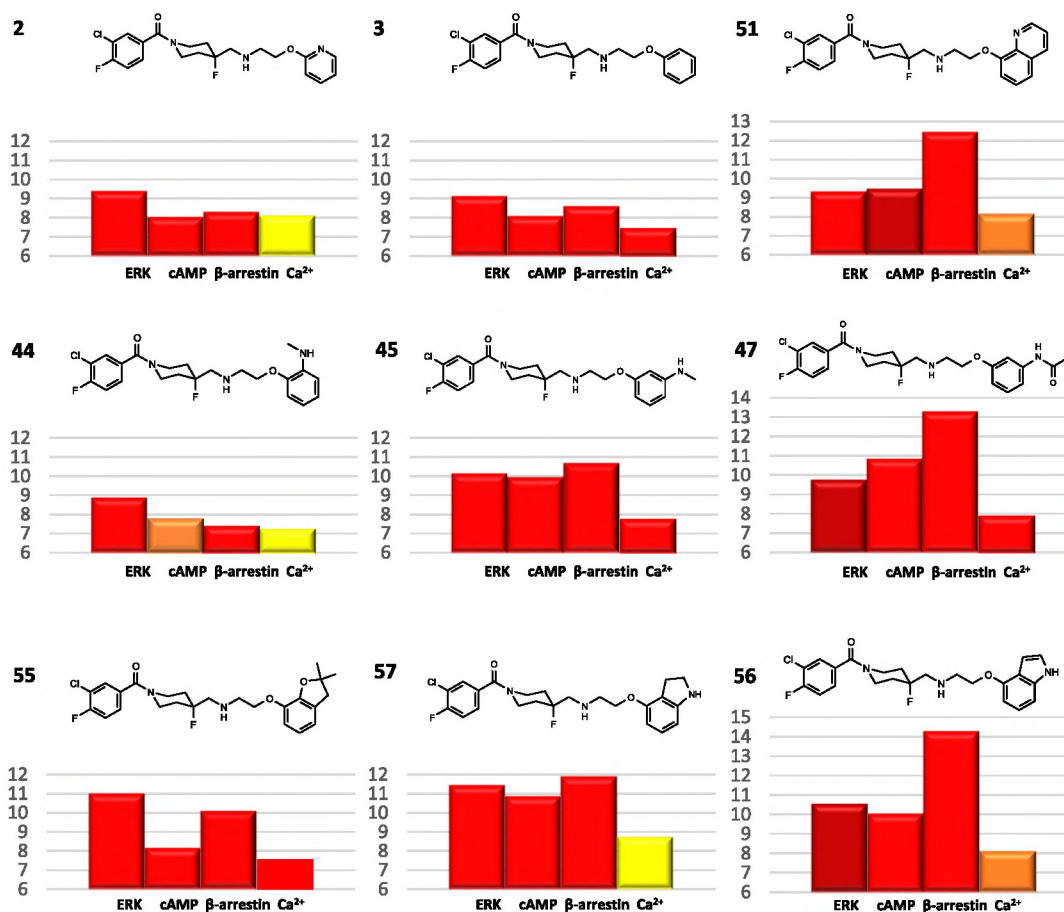


Figure 7. “Signaling fingerprints” for the novel compounds (bar height—normalized ligand potency in log scale, bar color—ligand efficacy, as percent E_{max}). The signaling fingerprints for 2 and 3 are shown for comparison with our previous work.¹³

41.7 mL/min/kg, respectively), similar to diazepam, a reference CNS drug with medium but acceptable stability, whereas compound 56 was more stable, with intrinsic clearance close to aripiprazole, a reference CNS drug showing a very high stability in this experimental setting (CL_{int} 9.6 and 7.2 mL/min/kg, respectively).

As a next step, compounds 44 and 56 were tested for membrane permeability using PAMPA and for potential hepatotoxicity using HepG2 cell viability (Table 7). Both compounds, similar to the lead structure 3, showed satisfying permeability ($>1 \times 10^{-6}$ cm/s), suggesting good absorption and brain penetration as well as very low hepatotoxicity, not reaching statistically significant reduction of viability even in a concentration as high as 50 μ M.

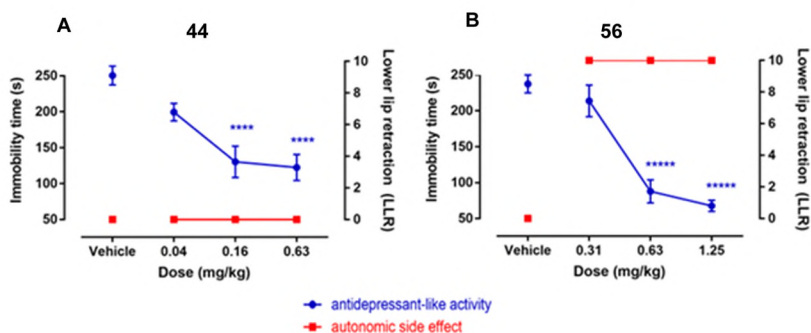
Table 7. Permeability, Hepatotoxicity, and Intrinsic Clearance of Compounds 3, 44, and 56

compound	PAMPA Pe [10^{-6} cm/s] \pm SD	hepatotoxicity 50% viability of HepG2 cells	intrinsic clearance CL_{int} [mL/min/kg]
3	8.6 ± 1.4	$>50 \mu$ M	41.7
44	6.7 ± 1.1	$>50 \mu$ M	48.8
56	4.7 ± 0.4	$>50 \mu$ M	9.6
references			
	Caffeine	Doxorubicin	diazepam
	15.1 ± 0.40	$<1 \mu$ M	31.0
	norfloxacin	CCCP	aripiprazole
	0.56 ± 0.13	$<10 \mu$ M	7.02

Finally, compounds 44 and 56 were tested for selectivity against a broad group of 45 off-targets, including those structurally and evolutionally closest to the 5-HT_{1A} receptor as well as the most troublesome for drug development (e.g., hERG channel, Chart 1, Supporting Information Tables S4 and S5). In most cases, the affinity for the off-targets proved to be in the micromolar range ($<50\%$ binding in 1×10^{-6}). For some of the targets, binding was stronger, but considering the very high affinity of the tested compounds for the 5-HT_{1A} receptor, the estimated selectivity was still over 3 orders of magnitude ($>1000\times$), even relatively higher than for the lead structure 3. Interestingly, compound 56, which displayed relatively highest affinity for some of the off-targets (reaching $pK_i \sim 8$), proved to be also relatively the most selective ($>10,000\times$) because of its extremely high affinity for the 5-HT_{1A} receptor ($pK_i = 12.80$). Based on all the data mentioned above, compounds 44 and 56 were ultimately selected for *in vivo* studies.

In Vivo Studies. So far, there is only sparse information connecting particular signaling transduction pathways with physiological effects. Evidence indicates that increased cortical ERK1/2 phosphorylation is associated with antidepressant activity,^{37,38} whereas inhibition of cAMP production by hippocampal 5-HT_{1A} receptors may interfere with memory process.^{39,40} On the other hand, it is currently not known what physiological effects are associated with activation of β -arrestin recruitment mediated by 5-HT_{1A} receptors. Nevertheless, it is very important for drug discovery to establish a link between

Chart 2. Differential Profiles in the FST (in Blue) and LLR (in Red) of Compounds 44 (A) and 56 (B), the 5-HT_{1A}R-Biased Agonists with Contrasting Functional Selectivity Signaling Fingerprints (Preferential for pERK1/2 and β -Arrestin, Respectively)^a



^a*****p* < 0.0001, ******p* < 0.00001.

particular functional profiles and the desired pharmacological effects.^{41,42} Therefore, two compounds with significantly differing *in vitro* functional pERK1/2 versus β -arrestin selectivity profiles were compared in various *in vivo* measures relevant to 5-HT_{1A} receptor agonism. Compound 44 has a pERK1/2 versus β -arrestin bias factor of 1.43 (*i.e.*, its EC₅₀ is almost 30-fold lower for ERK1/2 phosphorylation than for β -arrestin recruitment), while compound 56 has a bias factor of -3.49, translating to over 3000-fold greater potency for β -arrestin recruitment than for pERK1/2. Interestingly, while both compounds displayed similar effectiveness in the Porsolt forced swimming test (FST) for antidepressant activity, with 44 being slightly more potent (minimal effective dose MED = 0.16 mg/kg *p.o.* for 44 vs 0.63 mg/kg *p.o.* for 56), they differed significantly in their ability to induce lower lip retraction (LLR). LLR is an autonomic response, a component of the rat “serotonergic syndrome”, attributed to 5-HT_{1A} receptor activation.⁴³ Compound 44 did not induce any significant LLR, even up to a dose 4× higher than the MED for antidepressant activity, while compound 56 elicited a full LLR in a dose 2× lower than the MED in Porsolt test (Chart 2, Supporting Information Tables S6 and S8).

Noteworthy, at the time point that the *in vivo* effects were observed, we verified that there was a detectable exposure of the tested compounds in both serum and brain (Supporting Information Chart S1, Table S10). Moreover, the above-mentioned pharmacological effects were reversed by the selective 5-HT_{1A} receptor antagonist WAY100635, thus testifying for their full 5-HT_{1A} receptor dependence (Supporting Information Tables S7 and S9).

The significance of the LLR effect for human condition is so far unknown. However, it is undoubtedly an autonomic side effect, not connected with the antidepressant-like response in rat, and has previously been considered to be inseparable from the desired therapeutic-like effects resulting from the 5-HT_{1A} receptor activation.⁴⁴ Interestingly, antidepressant-like activity in the FST is mediated by activation of the cortical postsynaptic subpopulation of 5-HT_{1A} receptors, while induction of LLR is thought to be mediated by presynaptic 5-HT_{1A} autoreceptors localized in the Raphe nuclei.^{45,46} In the case of 5-HT_{1A} receptors, the contrasting roles of pre- and postsynaptic receptors in different brain regions have been extensively investigated, also in the context of therapeutic effectiveness.¹⁶ The diverse pharmacological profiles of 44 and 56 are therefore of considerable interest because they suggest that different preferences for β -arrestin recruitment relative to

ERK1/2 phosphorylation (functional selectivity at the cellular level) may be associated with preferential activation of particular subpopulations of 5-HT_{1A} receptors (brain region selectivity) and thus lead to separate therapeutic and side effects. It should also be considered that such a high level of β -arrestin-biased agonism, reported for the first time in the present study, could open the way to novel opportunities for targeting 5-HT_{1A} receptors, with previously unexplored physiological or behavioral outcomes. However, these are preliminary suggestions that need to be carefully and thoroughly evaluated using more numerous biased agonists and diversified technical approaches. Although these observations are promising and warrant further investigation, formal demonstration of superior therapeutic activity by biased agonists ultimately requires appropriately designed clinical trials and a clear understanding linking *in vitro* biased agonism to disease mechanisms. Nevertheless, the present work provides compelling evidence that chemical modifications of 5-HT_{1A} receptor-biased agonists allow for their functional diversification, which in turn translates to distinct pharmacological effects *in vivo*.

CONCLUSIONS

The present work describes the SARs and SFARs of 5-HT_{1A} receptor agonists and proves that novel and highly selective biased agonists can be designed to exhibit distinct and innovative signaling profiles. Thus, a series of 30 novel derivatives of 1-(1-benzoylpiperidin-4-yl)methanamine was synthesized and found to exhibit high affinity for the 5-HT_{1A} receptor ($pK_i > 8.0$, LLE > 5.0). Twenty-seven of these had subnanomolar affinities ($pK_i > 9.0$, LLE > 6) and 15 compounds possessed higher lipophilic-ligand efficiencies than the lead compound 3. Noteworthy, compound 56 was found to be extremely potent, one of the highest affinity 5-HT_{1A} receptor ligands discovered to date (based on the ChEMBL database). Moreover, most of the presented compounds showed substantial selectivity versus key anti-targets—the adrenergic α_1 and dopaminergic D₂ receptors (K_i ratio over 1000-fold). Twenty-five compounds were selected and tested in four functional assays connected with the 5-HT_{1A} receptor activation, that is, ERK1/2 phosphorylation (pERK1/2), adenylyl cyclase inhibition (cAMP), calcium mobilization (Ca²⁺), and β -arrestin recruitment. Based on analysis of SFARs and of bias factors, nine novel 5-HT_{1A} receptor-biased agonists were identified that exhibit diversified functional activity

profiles (i.e., “signaling fingerprints”). The selected, most interesting biased agonists **44** and **56** displayed high selectivity versus a panel of 45 off-target sites as well as promising metabolic stability, high permeability, and low hepatotoxicity, thus testifying for their favorable developability profiles. Strikingly, whereas **44** exhibited marked biased agonism for activation of pERK1/2, **56** exhibited the opposite profile, with very potent biased agonism for β -arrestin recruitment. The profile of **56** is, to our knowledge, unprecedented and could constitute a novel class of 5-HT_{1A} receptor-biased agonists, an interpretation reinforced by the differential *in vivo* activity of the two compounds in tests of antidepressant-like activity (FST) and behavioral syndrome (LLR). **44** preferentially elicited antidepressant-like effects, whereas **56** more potently elicited LLR, thus suggesting that the balance of β -arrestin recruitment relative to ERK1/2 phosphorylation (functional selectivity) may be associated with accentuated activity in specific physiological and/or behavioral models. As discussed previously, such differences likely reflect activation of particular subpopulations of the 5-HT_{1A} receptors (regional selectivity) and may account for differential separation of therapeutic and side effects.^{16,47,48} The novel 5-HT_{1A} agonists described herein, displaying diversified functional profiles, may constitute promising tool drugs to investigate the activity of 5-HT_{1A} receptor subpopulations and, potentially, could be developed as pharmacotherapeutics to treat CNS disorders involving dysfunctional serotonergic neurotransmission.

EXPERIMENTAL SECTION

Molecular Modeling. Computer-aided ligand design and further studies on SARs were based on ligand–receptor interaction analysis. The previously built template of the 5-HT_{1B} crystal structure (PDB ID 4IAR)⁴⁹ and preoptimized serotonin 5-HT_{1A} receptor homology model served as a structural target for docking studies.⁵⁰ To capture distinctive binding mode of a variety of functionally biased ligands, the general procedure for developing ligand-optimized models using induced-fit technique⁵¹ served as both a ligand-steered binding site optimization method (in terms of amino acid side chains) and a routine docking approach, predicting bioactive conformation.¹³ Glide SP flexible docking procedure using an OPLS3 force field was set for the induced-fit docking (IFD). H-bond constraint and centroid of a grid box for docking to the 5-HT_{1A} receptor were located on Asp3.32. Ligand structures were sketched in Maestro 2D Sketcher and optimized using a LigPrep tool. The aforementioned tools were implemented in Small-Molecule Drug Discovery Suite (Schrodinger, Inc. New York, USA), which was licensed for Jagiellonian University Medical College. Instant JChem was used for structure database management and property prediction, Instant JChem 20.8.0, 2020, ChemAxon (<http://www.chemaxon.com>).

Chemistry. General Chemistry Information. All the reagents were purchased from commercial suppliers (Sigma-Aldrich, Merck, Chempur, Fluorochem, Enamine, Acros Organics, Manchester Organics, POCh, Activate Scientific, Chem-Impex International, Apollo Scientific) and were used without further purification. Analytical thin-layer chromatography was performed on Merck Kieselgel 60 F₂₅₄ (0.25 mm) precoated aluminum sheets (Merck, Darmstadt, Germany). Compounds were visualized with UV light and by suitable visualization reagents 2.9% solution of ninhydrin in a mixture of 1-propanol and acetic acid (100/3, v/v) and Pancaldi reagent [solution of 12.0 g (NH₄)₆Mo₇O₂₄, 0.5 g Ce(SO₄)₂ and 6.8 mL of 98% H₂SO₄ in 240 mL of water]. Flash chromatography was performed on CombiFlash RF (Teledyne Isco) using disposable silica gel flash columns RediSep Rf (silica gel 60, particle size 40–63 μ m) and RediSep Gold (silica gel 60, particle size 20–40 μ m) purchased from Teledyne Isco. The ultraperformance liquid chromatography (UPLC)–mass spectrometry (MS) or UPLC–tandem mass spec-

trometry (MS/MS) analysis was done on a UPLC–MS/MS system comprising a Waters ACQUITY UPLC (Waters Corporation, Milford, MA, USA) coupled with a Waters tandem quadrupole (TQD) mass spectrometer (electrospray ionization (ESI) mode with TQD). Chromatographic separations were carried out using the ACQUITY UPLC BEH (bridged ethyl hybrid) C18 column: 2.1 \times 100 mm and 1.7 μ m particle size. The column was maintained at 40 °C and eluted under gradient conditions using 95–0% of eluent A over 10 min at a flow rate of 0.3 mL/min. Eluent A: 0.1% solution of formic acid in water (v/v); eluent B: 0.1% solution of formic acid in acetonitrile (v/v). A total of 10 μ L of each sample was injected and chromatograms were recorded using a Waters e_l photodiode array detector. The spectra were analyzed in the range of 200–700 nm with 1.2 nm resolution and at a sampling rate of 20 points/s. The UPLC–MS purity of all the test compounds and key intermediates were determined to be >95%. ¹H NMR, ¹³C NMR, and ¹⁹F NMR spectra were obtained in a Varian Mercury spectrometer (Varian Inc., Palo Alto, CA, USA) and JEOL spectrometer (JEOL SAS., Tokyo, Japan), in CDCl₃, CD₃OD, or DMSO-*d*₆ operating at 300 MHz (¹H NMR), 75 MHz or 126 MHz (¹³C NMR), and 282 MHz (¹⁹F NMR). Chemical shifts are reported as δ values (ppm) relative to TMS δ = 0 (¹H) as internal standard (IS). The *J* values are expressed in Hertz (Hz). Signal multiplicities are represented by the following abbreviations: s (singlet), br s (broad singlet), bd (broad doublet), d (doublet), dd (doublet of doublets), dt (doublet of triplets), t (triplet), td (triplet of doublets), tdd (triplet of doublet of doublets), q (quartet), dq (doublet of quartets), and m (multiplet). Melting points were determined on a Büchi Melting Point B-540 apparatus using open glass capillaries and are uncorrected.

Synthetic Procedures. Previously reported or commercially available compounds:

2-(1-(3-Chloro-4-fluorobenzoyl)-4-fluoropiperidin-4-yl)-2-hydroxyacetonitrile (**4**),¹³

2-(1-(3,4-Dichlorobenzoyl)-4-fluoropiperidin-4-yl)-2-hydroxyacetonitrile (**5**),¹³

2-(2-Chlorophenoxy)ethanamine (**9**).

Detailed Procedures for the Preparation of the Amine Intermediates 6–26 Are Described in the Supporting Information. General Procedures for the Preparation of 1-(1-Benzoylpiperidin-4-yl)methanamine Derivatives (27–57). To appropriate cyanohydrin (**4** or **5**)¹³ (1.0 equiv) dissolved in methanol, DABCO (2.0–12.5 equiv) was added in one portion, followed by the appropriate amine (**6–26**) (1.0–1.6 equiv), 4 c $\bar{5}$ molecular sieves, sodium cyanoborohydride (1.6–7.8 equiv), and iron sulfate heptahydrate (FeSO₄ \times 7 H₂O) (1.1 equiv). The mixture was stirred at room temperature until the cyanohydrin was consumed (24–72 h); then, the reaction mixture was filtered, concentrated *in vacuo*, and next brine was added. The resulting mixture was extracted with EtOAc (3 \times), organics were combined and dried over magnesium sulfate, filtered, and concentrated. The crude product was purified by flash chromatography.

tert-Butyl (3-(2-(((1-(3-Chloro-4-fluorobenzoyl)-4-fluoropiperidin-4-yl)methyl)amino)ethoxy)phenyl)(methyl)carbamate (**27**). The title compound was prepared using 2-(1-(3-chloro-4-fluorobenzoyl)-4-fluoropiperidin-4-yl)-2-hydroxyacetonitrile (**4**) (0.110 g, 0.35 mmol) *tert*-butyl (3-(2-aminoethoxy)phenyl)(methyl)carbamate (**17**) (0.120 g, 0.45 mmol), DABCO (0.487 g, 4.34 mmol), sodium cyanoborohydride (0.167 g, 2.71 mmol), molecular sieves (0.900 g), and iron sulfate heptahydrate (0.106 g, 0.38 mmol) in methanol (5 mL). Purification: DCM/methanol/NH₃(aq) (9.5/0.5/0.02, v/v/v). Yield: 40%; colorless oil. ¹H NMR (300 MHz, CDCl₃, δ): 7.48 (dd, *J* = 1.8, 7.0 Hz, 1H), 7.33–7.25 (m, 1H), 7.19 (td, *J* = 8.3, 11.6 Hz, 2H), 6.86–6.77 (m, 2H), 6.74–6.65 (m, 1H), 4.51 (br s, 1H), 4.04 (t, *J* = 5.3 Hz, 2H), 3.58 (br s, 1H), 3.35 (br s, 1H), 3.23 (s, 3H), 3.20–3.08 (m, 1H), 3.02 (t, *J* = 5.0 Hz, 2H), 2.91–2.75 (m, 2H), 2.00 (br s, 2H), 1.64 (br s, 3H), 1.45 (s, 9H). Formula: C₂₇H₃₄ClF₂N₃O₄; MS (ESI⁺) *m/z*: 538 [M + H⁺].

(3-Chloro-4-fluorophenyl)(4-fluoro-4-(((2-(2-fluorophenoxy)ethyl)amino)methyl)piperidin-1-yl)methanone (**28**). The title compound was prepared using 2-(1-(3-chloro-4-fluorobenzoyl)-4-fluoro-

piperidin-4-yl)-2-hydroxyacetonitrile (**4**) (0.150 g, 0.48 mmol), 2-(2-fluorophenoxy)ethanamine (**6**) (0.118 g, 0.76 mmol), DABCO (0.669 g, 5.97 mmol), sodium cyanoborohydride (0.234 g, 3.73 mmol), molecular sieves (1.043 g), and iron sulfate heptahydrate (0.146 g, 0.53 mmol) in methanol (5 mL). Purification: EtOAc/methanol (9.5/0.5, v/v). Yield: 72%; pale yellow crystallizing oil. ^1H NMR (300 MHz, CDCl_3 , δ): 7.51–7.45 (m, 1H), 7.33–7.25 (m, 1H), 7.21–7.13 (m, 1H), 7.11–7.01 (m, 2H), 7.01–6.86 (m, 2H), 4.50 (br s, 1H), 4.13 (t, $J = 5.0$ Hz, 2H), 3.58 (br s, 1H), 3.47–3.14 (m, 2H), 3.05 (t, $J = 5.0$ Hz, 2H), 2.86 (d, $J = 19.9$ Hz, 2H), 2.00 (s, 2H), 1.83–1.51 (m, 3H). ^{13}C NMR (75 MHz, CDCl_3 , δ): 168.0, 158.8 (d, $J = 254$ Hz), 152.8 (d, $J = 246.4$ Hz), 146.8 (d, $J = 10.4$ Hz), 132.9 (d, $J = 4.6$ Hz), 129.7, 127.1 (d, $J = 6.9$ Hz), 124.3 (d, $J = 3.5$ Hz), 121.5 (d, $J = 18.4$ Hz), 121.5 (d, $J = 6.9$ Hz), 116.8 (d, $J = 22$ Hz), 116.3 (d, $J = 18.4$ Hz), 115.3, 94.4 (d, $J = 172$ Hz), 69.2, 57.2 (d, $J = 22$ Hz), 49.2, 43.6, 38.2, 33.4, 32.6. Formula: $\text{C}_{21}\text{H}_{22}\text{ClF}_3\text{N}_2\text{O}_2$; MS (ESI⁺) m/z : 427 [$\text{M} + \text{H}^+$].

(3-Chloro-4-fluorophenyl)(4-fluoro-4-(((2-(3-fluorophenoxy)ethyl)amino)methyl)piperidin-1-yl)methanone (**29**). The title compound was prepared using 2-(1-(3-chloro-4-fluorobenzoyl)-4-fluoropiperidin-4-yl)-2-hydroxyacetonitrile (**4**) (0.150 g, 0.48 mmol), 2-(3-fluorophenoxy)ethanamine (**7**) (0.118 g, 0.76 mmol), DABCO (0.669 g, 5.97 mmol), sodium cyanoborohydride (0.234 g, 3.73 mmol), molecular sieves (1.043 g), and iron sulfate heptahydrate (0.146 g, 0.53 mmol) in methanol (5 mL). Purification: *n*-hexane/EtOAc/methanol/ $\text{NH}_3(\text{aq})$ (5/4.5/0.5/0.02, v/v/v/v). Yield: 40%; white crystallizing oil. ^1H NMR (300 MHz, CDCl_3 , δ): 7.48 (dd, $J = 2.1, 6.9$ Hz, 1H), 7.33–7.26 (m, 1H), 7.24–7.13 (m, 2H), 6.67 (td, $J = 1.0, 2.0, 9.5$ Hz, 2H), 6.64–6.58 (m, 1H), 4.51 (br s, 1H), 4.04 (t, $J = 5.0$ Hz, 2H), 3.60 (br s, 1H), 3.46–3.10 (m, 2H), 3.03 (t, $J = 5.1$ Hz, 2H), 2.90–2.77 (m, 2H), 2.01 (br s, 2H), 1.63 (br s, 3H). ^{13}C NMR (75 MHz, CDCl_3 , δ): 168.1, 163.6 (d, $J = 245$ Hz), 160.1 (d, $J = 11.1$ Hz), 158.8 (d, $J = 254$ Hz), 132.9 (d, $J = 4.4$ Hz), 130.2 (d, $J = 10$ Hz), 129.7, 127.1 (d, $J = 7.7$ Hz), 121.5 (d, $J = 18.2$ Hz), 116.8 (d, $J = 22$ Hz), 110.2 (d, $J = 2.8$ Hz), 107.7 (d, $J = 22$ Hz), 102.2 (d, $J = 24$ Hz), 94.4 (d, $J = 172$ Hz), 67.7, 57.3 (d, $J = 22$ Hz), 49.1, 43.9, 38.6, 33.5, 32.8. Formula: $\text{C}_{21}\text{H}_{22}\text{ClF}_3\text{N}_2\text{O}_2$; MS (ESI⁺) m/z : 427 [$\text{M} + \text{H}^+$].

(3,4-Dichlorophenyl)(4-fluoro-4-(((2-(3-fluorophenoxy)ethyl)amino)methyl)piperidin-1-yl)methanone (**30**). The title compound was prepared using 2-(1-(3,4-dichlorobenzoyl)-4-fluoropiperidin-4-yl)-2-hydroxyacetonitrile (**5**) (0.150 g, 0.45 mmol), 2-(3-fluorophenoxy)ethanamine (**7**) (0.064 g, 0.41 mmol), DABCO (0.634 g, 5.66 mmol), sodium cyanoborohydride (0.034 g, 0.54 mmol), molecular sieves (0.500 g), and iron sulfate heptahydrate (0.137 g, 0.50 mmol) in methanol (8 mL). Purification: *n*-hexane/ Et_2O /DCM/methanol/ $\text{NH}_3(\text{aq})$ (2/2/5.5/0.5/0.02, v/v/v/v/v). Yield: 35%; yellow transparent oil. ^1H NMR (300 MHz, CDCl_3 , δ): 7.57–7.42 (m, 2H), 7.26–7.17 (m, 2H), 6.73–6.55 (m, 3H), 4.52 (br s, 1H), 4.04 (t, $J = 5.1$ Hz, 2H), 3.59 (br s, 1H), 3.44–3.10 (m, 2H), 3.03 (t, $J = 5.0$ Hz, 2H), 2.91–2.75 (m, 2H), 2.01 (br s, 2H), 1.62 (br s, 3H). ^{13}C NMR (75 MHz, CDCl_3 , δ): 167.9, 163.6 (d, $J = 245.4$ Hz), 160.1 (d, $J = 10.4$ Hz), 135.6, 134.1, 133.0, 130.6, 130.2 (d, $J = 10.4$ Hz), 129.1, 126.2, 110.2 (d, $J = 2.3$ Hz), 107.7 (d, $J = 20$ Hz), 102.2 (d, $J = 24$ Hz), 94.3 (d, $J = 172$ Hz), 67.6, 57.3 (d, $J = 22$ Hz), 49.1, 43.5, 38.2, 33.4, 32.6. Formula: $\text{C}_{21}\text{H}_{22}\text{Cl}_2\text{F}_2\text{N}_2\text{O}_2$; MS (ESI⁺) m/z : 443 [$\text{M} + \text{H}^+$].

(3-Chloro-4-fluorophenyl)(4-fluoro-4-(((2-(4-fluorophenoxy)ethyl)amino)methyl)piperidin-1-yl)methanone (**31**). The title compound was prepared using 2-(1-(3-chloro-4-fluorobenzoyl)-4-fluoropiperidin-4-yl)-2-hydroxyacetonitrile (**4**) (0.100 g, 0.32 mmol), 2-(4-fluorophenoxy)ethanamine (**8**) (0.074 g, 0.48 mmol), DABCO (0.444 g, 3.97 mmol), sodium cyanoborohydride (0.155 g, 2.48 mmol), molecular sieves (0.900 g), and iron sulfate heptahydrate (0.097 g, 0.35 mmol) in methanol (4 mL). Purification: *n*-hexane/EtOAc/methanol/ $\text{NH}_3(\text{aq})$ (6/3.5/0.5/0.02, v/v/v/v). Yield: 64%; white crystallizing oil. ^1H NMR (300 MHz, CDCl_3 , δ): 7.48 (dd, $J = 2.3, 7.0$ Hz, 1H), 7.33–7.24 (m, 1H), 7.22–7.11 (m, 1H), 7.01–6.90 (m, 2H), 6.88–6.78 (m, 2H), 4.51 (br s, 1H), 4.02 (t, $J = 5.3$ Hz, 2H), 3.62 (d, $J = 19.3$ Hz, 1H), 3.48–3.10 (m, 2H), 3.01 (t, $J = 5.0$

Hz, 2H), 2.83 (d, $J = 19.9$ Hz, 2H), 2.06–1.94 (m, 2H), 1.83–1.45 (m, 3H). ^{13}C NMR (75 MHz, CDCl_3 , δ): 168.1, 158.8 (d, $J = 253$ Hz), 157.3 (d, $J = 238$ Hz), 154.9, 132.9 (d, $J = 4.6$ Hz), 129.7, 127.1 (d, $J = 6.9$ Hz), 121.5 (d, $J = 18.4$ Hz), 116.8 (d, $J = 22$ Hz), 115.8 (d, $J = 23$ Hz, 2C), 115.5 (d, $J = 8.1$ Hz, 2C), 94.3 (d, $J = 172$ Hz), 68.0, 57.3 (d, $J = 22$ Hz), 49.3, 43.7, 38.3, 33.6, 32.7. Formula: $\text{C}_{21}\text{H}_{22}\text{ClF}_3\text{N}_2\text{O}_2$; MS (ESI⁺) m/z : 427 [$\text{M} + \text{H}^+$].

(3-Chloro-4-fluorophenyl)(4-fluoro-4-(((2-(2-chlorophenoxy)ethyl)amino)methyl)piperidin-1-yl)methanone (**32**). The title compound was prepared using 2-(1-(3-chloro-4-fluorobenzoyl)-4-fluoropiperidin-4-yl)-2-hydroxyacetonitrile (**4**) (0.150 g, 0.48 mmol), 2-(2-chlorophenoxy)ethanamine (**9**) (0.131 g, 0.76 mmol), DABCO (0.669 g, 5.97 mmol), sodium cyanoborohydride (0.234 g, 3.73 mmol), molecular sieves (1.043 g), and iron sulfate heptahydrate (0.146 g, 0.53 mmol) in methanol (5 mL). Purification: DCM/methanol (9.5/0.5/0.02, v/v/v) and then *n*-hexane/EtOAc/methanol/ $\text{NH}_3(\text{aq})$ (6/3.5/0.5/0.02, v/v/v/v). Yield: 48%; beige crystallizing oil. ^1H NMR (300 MHz, CDCl_3 , δ): 7.47 (dd, $J = 1.8, 7.0$ Hz, 1H), 7.35 (d, $J = 1.8, 7.6$ Hz, 1H), 7.32–7.26 (m, 1H), 7.24–7.12 (m, 2H), 6.96–6.84 (m, 2H), 4.49 (br s, 1H), 4.12 (t, $J = 5.0$ Hz, 2H), 3.59 (d, $J = 5.9$ Hz, 1H), 3.45–3.12 (m, 2H), 3.07 (t, $J = 5.0$ Hz, 2H), 2.95–2.80 (m, 2H), 2.00 (br s, 2H), 1.84 (s, 1H), 1.77–1.53 (m, 2H). ^{13}C NMR (75 MHz, CDCl_3 , δ): 168.0, 158.8 (d, $J = 254$ Hz), 154.2, 132.9 (d, $J = 4.6$ Hz), 130.3, 129.7, 127.8, 127.1 (d, $J = 6.9$ Hz), 123.0, 121.7, 121.5 (d, $J = 18.4$ Hz), 116.8 (d, $J = 22$ Hz), 113.7, 94.4 (d, $J = 172$ Hz), 68.9, 57.2 (d, $J = 22$ Hz), 49.0, 43.7, 38.2, 33.5, 32.7. Formula: $\text{C}_{21}\text{H}_{22}\text{Cl}_2\text{F}_2\text{N}_2\text{O}_2$; MS (ESI⁺) m/z : 443 [$\text{M} + \text{H}^+$].

(3-Chloro-4-fluorophenyl)(4-(((2-(3-chlorophenoxy)ethyl)amino)methyl)-4-fluoropiperidin-1-yl)methanone (**33**). The title compound was prepared using 2-(1-(3-chloro-4-fluorobenzoyl)-4-fluoropiperidin-4-yl)-2-hydroxyacetonitrile (**4**) (0.150 g, 0.48 mmol), 2-(3-chlorophenoxy)ethanamine (**10**) (0.131 g, 0.76 mmol), DABCO (0.669 g, 5.97 mmol), sodium cyanoborohydride (0.234 g, 3.73 mmol), molecular sieves (1.043 g), and iron sulfate heptahydrate (0.146 g, 0.53 mmol) in methanol (5 mL). Purification: *n*-hexane/EtOAc/methanol/ $\text{NH}_3(\text{aq})$ (5/4.5/0.5/0.02, v/v/v/v). Yield: 28%; beige crystallizing oil. ^1H NMR (300 MHz, CDCl_3 , δ): 7.48 (dd, $J = 2.1, 6.9$ Hz, 1H), 7.33–7.26 (m, 1H), 7.18 (dt, $J = 5.1, 8.3$ Hz, 2H), 6.96–6.91 (m, 1H), 6.90 (t, $J = 2.1$ Hz, 1H), 6.78 (ddd, $J = 0.8, 2.4, 8.3$ Hz, 1H), 4.52 (br s, 1H), 4.04 (t, $J = 5.0$ Hz, 2H), 3.60 (br s, 1H), 3.37 (br s, 2H), 3.02 (t, $J = 5.1$ Hz, 2H), 2.90–2.77 (m, 2H), 2.02 (br s, 2H), 1.63 (s, 3H). ^{13}C NMR (75 MHz, CDCl_3 , δ): 168.1, 159.5, 158.8 (d, $J = 254$ Hz), 134.9, 132.9 (d, $J = 4.4$ Hz), 130.2, 129.7, 127.1 (d, $J = 7.7$ Hz), 121.7, 121.1, 116.8 (d, $J = 22$ Hz), 114.9, 113.0, 94.3 (d, $J = 172$ Hz), 67.6, 57.3 (d, $J = 22$ Hz), 49.1, 43.3, 39.6, 33.3 (2C). Formula: $\text{C}_{21}\text{H}_{22}\text{Cl}_2\text{F}_2\text{N}_2\text{O}_2$; MS (ESI⁺) m/z : 443 [$\text{M} + \text{H}^+$].

4-(((2-(3-Chlorophenoxy)ethyl)amino)methyl)-4-fluoropiperidin-1-yl)(3,4-dichlorophenyl)methanone (**34**). The title compound was prepared using 2-(1-(3,4-dichlorobenzoyl)-4-fluoropiperidin-4-yl)-2-hydroxyacetonitrile (**4**) (0.150 g, 0.45 mmol), 2-(3-chlorophenoxy)ethanamine (**10**) (0.070 g, 0.41 mmol), DABCO (0.634 g, 5.66 mmol), sodium cyanoborohydride (0.034 g, 0.54 mmol), molecular sieves (0.500 g), and iron sulfate heptahydrate (0.137 g, 0.50 mmol) in methanol (8 mL). Purification: *n*-hexane/EtOAc/methanol/ $\text{NH}_3(\text{aq})$ (4/5.5/0.5/0.02, v/v/v/v). Yield: 36%; yellow oil. ^1H NMR (300 MHz, CDCl_3 , δ): 7.53–7.46 (m, 2H), 7.25–7.15 (m, 2H), 6.97–6.87 (m, 2H), 6.78 (ddd, $J = 1.0, 2.4, 8.3$ Hz, 1H), 4.52 (br s, 1H), 4.04 (t, $J = 5.1$ Hz, 2H), 3.59 (br s, 1H), 3.46–3.12 (m, 2H), 3.02 (t, $J = 5.1$ Hz, 2H), 2.91–2.76 (m, 2H), 2.00 (d, $J = 12.3$ Hz, 2H), 1.61 (br s, 3H). ^{13}C NMR (75 MHz, CDCl_3 , δ): 167.9, 159.5, 135.6, 134.9, 134.1, 133.0, 130.6, 130.2, 129.1, 126.2, 121.1, 114.9, 113.0, 94.3 (d, $J = 172$ Hz), 67.6, 57.2 (d, $J = 22$ Hz), 49.1, 43.5, 38.2, 33.5, 32.9. Formula: $\text{C}_{21}\text{H}_{22}\text{Cl}_3\text{FN}_2\text{O}_2$; MS (ESI⁺) m/z : 459 [$\text{M} + \text{H}^+$].

(3-Chloro-4-fluorophenyl)(4-fluoro-4-(((2-(4-chlorophenoxy)ethyl)amino)methyl)piperidin-1-yl)methanone (**35**). The title compound was prepared using 2-(1-(3-chloro-4-fluorobenzoyl)-4-fluoropiperidin-4-yl)-2-hydroxyacetonitrile (**4**) (0.100 g, 0.32 mmol), 2-(4-chlorophenoxy)ethanamine (**11**) (0.082 g, 0.48 mmol), DABCO

(0.444 g, 3.97 mmol), sodium cyanoborohydride (0.155 g, 2.48 mmol), molecular sieves (0.900 g), and iron sulfate heptahydrate (0.097 g, 0.35 mmol) in methanol (4 mL). Purification: *n*-hexane/EtOAc/methanol/ $\text{NH}_3(\text{aq})$ (6/3.5/0.5/0.02, v/v/v/v). Yield: 64%; white oil. ^1H NMR (300 MHz, CDCl_3 , δ): 7.48 (dd, J = 2.1, 6.7 Hz, 1H), 7.34–7.12 (m, 4H), 6.87–6.77 (m, 2H), 4.50 (br s, 1H), 4.02 (t, J = 5.0 Hz, 2H), 3.74–3.49 (m, 1H), 3.24 (br s, 2H), 3.02 (t, J = 5.0 Hz, 2H), 2.91–2.74 (m, 2H), 2.00 (br s, 2H), 1.88–1.44 (m, 3H). ^{13}C NMR (75 MHz, CDCl_3 , δ): 168.1, 157.4, 158.8 (d, J = 254 Hz), 132.9 (d, J = 4.6 Hz), 129.7, 129.3 (2C), 127.1 (d, J = 6.9 Hz), 125.8, 121.5 (d, J = 18.4 Hz), 116.8 (d, J = 22 Hz), 115.7 (2C), 94.3 (d, J = 172 Hz), 67.7, 57.3 (d, J = 22 Hz), 49.2, 43.7, 38.3, 33.6, 32.8. Formula: $\text{C}_{21}\text{H}_{22}\text{Cl}_2\text{F}_2\text{N}_2\text{O}_2$; MS (ESI⁺) m/z : 443 [M + H⁺].

(3-Chloro-4-fluorophenyl)(4-fluoro-4-(((2-(2-methoxyphenoxy)ethyl)amino)methyl)piperidin-1-yl)methanone (36). The title compound was prepared using 2-(1-(3-chloro-4-fluorobenzoyl)-4-fluoropiperidin-4-yl)-2-hydroxyacetonitrile (4) (0.505 g, 1.61 mmol), 2-(2-methoxyphenoxy)ethanamine (12) (0.430 g, 2.58 mmol), DABCO (2.256 g, 20.11 mmol), sodium cyanoborohydride (0.788 g, 12.55 mmol), and molecular sieves (3.300 g) in methanol (15 mL). Purification: *n*-hexane/EtOAc/methanol/ $\text{NH}_3(\text{aq})$ (6/3.5/0.5/0.02, v/v/v/v). Yield: 35%; pale yellow crystallizing oil. ^1H NMR (300 MHz, CDCl_3 , δ): 7.48 (dd, J = 2.1, 6.9 Hz, 1H), 7.32–7.26 (m, 1H), 7.20–7.13 (m, 1H), 6.98–6.85 (m, 4H), 4.50 (br s, 1H), 4.12 (t, J = 5.3 Hz, 2H), 3.84 (s, 3H), 3.60 (br s, 1H), 3.45–3.13 (m, 2H), 3.04 (t, J = 5.3 Hz, 2H), 2.91–2.79 (m, 2H), 2.10–1.92 (m, 2H), 1.70 (br s, 3H). ^{19}F NMR (282 MHz, CDCl_3 , δ): –112.7 (s, 1F), –166.3 (s, 1F). ^{13}C NMR (75 MHz, CDCl_3 , δ): 168.0, 158.8 (d, J = 245 Hz), 149.8, 148.2, 132.9 (d, J = 4.4 Hz), 129.7, 127.1 (d, J = 7.7 Hz), 121.6, 121.4, 120.9, 116.8 (d, J = 22 Hz), 114.2, 111.9, 94.4 (d, J = 172 Hz), 69.0, 57.3 (d, J = 22 Hz), 55.8, 49.3, 43.8, 38.3, 33.6, 32.8. Formula: $\text{C}_{22}\text{H}_{25}\text{ClF}_2\text{N}_2\text{O}_3$; MS (ESI⁺) m/z : 439 [M + H⁺].

(3,4-Dichlorophenyl)(4-fluoro-4-(((2-(2-methoxyphenoxy)ethyl)amino)methyl)piperidin-1-yl)methanone (37). The title compound was prepared using 2-(1-(3,4-dichlorobenzoyl)-4-fluoropiperidin-4-yl)-2-hydroxyacetonitrile (5) (0.350 g, 1.06 mmol), 2-(2-methoxyphenoxy)ethanamine (12) (0.282 g, 1.69 mmol), DABCO (1.479 g, 13.18 mmol), sodium cyanoborohydride (0.518 g, 8.25 mmol), and molecular sieves (2.194 g) in methanol (10 mL). Purification: *n*-hexane/EtOAc/methanol/ $\text{NH}_3(\text{aq})$ (6/3.5/0.5/0.02, v/v/v/v). Yield: 30%; pale yellow crystallizing oil. ^1H NMR (300 MHz, CDCl_3 , δ): 7.53–7.45 (m, 2H), 7.23 (dd, J = 1.8, 8.2 Hz, 1H), 6.99–6.84 (m, 4H), 4.51 (br s, 1H), 4.12 (t, J = 5.3 Hz, 2H), 3.84 (s, 3H), 3.57 (br s, 1H), 3.46–3.10 (m, 2H), 3.04 (t, J = 5.1 Hz, 2H), 2.91–2.78 (m, 2H), 2.00 (br s, 2H), 1.77 (br s, 3H). ^{13}C NMR (75 MHz, CDCl_3 , δ): 167.9, 149.7, 148.2, 135.7, 134.1, 133.0, 130.6, 129.1, 126.2, 121.6, 120.9, 114.2, 111.9, 94.3 (d, J = 172 Hz), 69.0, 57.3 (d, J = 22 Hz), 55.8, 49.3, 43.6, 38.2, 33.4, 32.7. Formula: $\text{C}_{22}\text{H}_{25}\text{Cl}_2\text{FN}_2\text{O}_3$; MS (ESI⁺) m/z : 455 [M + H⁺].

(3-Chloro-4-fluorophenyl)(4-fluoro-4-(((2-(3-methoxyphenoxy)ethyl)amino)methyl)piperidin-1-yl)methanone (38). The title compound was prepared using 2-(1-(3-chloro-4-fluorobenzoyl)-4-fluoropiperidin-4-yl)-2-hydroxyacetonitrile (4) (0.165 g, 0.52 mmol), 2-(3-methoxyphenoxy)ethanamine (13) (0.140 g, 0.84 mmol), DABCO (0.734 g, 6.55 mmol), sodium cyanoborohydride (0.256 g, 4.09 mmol), molecular sieves (1.043 g), and iron sulfate heptahydrate (0.165 g, 0.58 mmol) in methanol (5 mL). Purification: *n*-hexane/EtOAc/methanol/ $\text{NH}_3(\text{aq})$ (8/1.5/0.5/0.02, v/v/v/v). Yield: 40%; yellow transparent oil. ^1H NMR (300 MHz, CDCl_3 , δ): 7.48 (dd, J = 2.1, 6.9 Hz, 1H), 7.33–7.26 (m, 1H), 7.21–7.13 (m, 2H), 6.54–6.48 (m, 2H), 6.47–6.45 (m, 1H), 4.52 (br s, 1H), 4.05 (t, J = 5.1 Hz, 2H), 3.78 (s, 3H), 3.59 (br s, 1H), 3.45–3.11 (m, 2H), 3.02 (t, J = 5.0 Hz, 2H), 2.91–2.76 (m, 2H), 2.01 (br s, 2H), 1.71 (br s, 3H). ^{13}C NMR (75 MHz, CDCl_3 , δ): 168.1, 160.8, 160.0, 158.8 (d, J = 254 Hz), 132.9 (d, J = 4.4 Hz), 129.9, 129.7, 127.1 (d, J = 7.7 Hz), 121.5 (d, J = 18.2 Hz), 116.8 (d, J = 22 Hz), 106.7, 106.4, 101.0, 94.3 (d, J = 172 Hz), 67.3, 57.3 (d, J = 22 Hz), 55.3, 49.3, 43.6, 38.2, 33.6, 32.8. Formula: $\text{C}_{22}\text{H}_{25}\text{ClF}_2\text{N}_2\text{O}_3$; MS (ESI⁺) m/z : 439 [M + H⁺].

(3,4-Dichlorophenyl)(4-fluoro-4-(((2-(3-methoxyphenoxy)ethyl)amino)methyl)piperidin-1-yl)methanone (39). The title compound

was prepared using 2-(1-(3,4-dichlorobenzoyl)-4-fluoropiperidin-4-yl)-2-hydroxyacetonitrile (5) (0.124 g, 0.37 mmol), 2-(3-methoxyphenoxy)ethanamine (13) (0.100 g, 0.60 mmol), DABCO (0.524 g, 4.68 mmol), sodium cyanoborohydride (0.183 g, 2.91 mmol), and molecular sieves (0.776 g) in methanol (4 mL). Purification: *n*-hexane/EtOAc/methanol/ $\text{NH}_3(\text{aq})$ (8/1.5/0.5/0.02, v/v/v/v). Yield: 30%; yellow oil. ^1H NMR (300 MHz, CDCl_3 , δ): 7.53–7.47 (m, 2H), 7.23 (dd, J = 1.8, 8.2 Hz, 1H), 7.18 (t, J = 8.1 Hz, 1H), 6.56–6.43 (m, 3H), 4.51 (br s, 1H), 4.05 (t, J = 5.1 Hz, 2H), 3.79 (s, 3H), 3.60 (br s, 1H), 3.38 (br s, 2H), 3.02 (t, J = 5.0 Hz, 2H), 2.90–2.78 (m, 2H), 2.01 (br s, 2H), 1.59 (br s, 3H). ^{13}C NMR (126 MHz, CDCl_3 , δ): 168.0, 160.9, 160.1, 135.7, 134.2, 133.1, 130.7, 130.0, 129.2, 126.3, 106.8, 106.5, 101.1, 94.4 (d, J = 172.6 Hz), 67.4, 57.4 (d, J = 21.7 Hz), 55.4, 49.4, 43.7, 38.2, 33.7 (d, J = 22.9 Hz), 32.8 (d, J = 21.1 Hz). Formula: $\text{C}_{22}\text{H}_{25}\text{Cl}_2\text{FN}_2\text{O}_3$; MS (ESI⁺) m/z : 455 [M + H⁺].

(3-Chloro-4-fluorophenyl)(4-fluoro-4-(((2-(4-methoxyphenoxy)ethyl)amino)methyl)piperidin-1-yl)methanone (40). The title compound was prepared using 2-(1-(3-chloro-4-fluorobenzoyl)-4-fluoropiperidin-4-yl)-2-hydroxyacetonitrile (4) (0.150 g, 0.48 mmol), 2-(4-methoxyphenoxy)ethanamine (14) (0.128 g, 0.77 mmol), DABCO (0.669 g, 5.97 mmol), sodium cyanoborohydride (0.234 g, 3.73 mmol), molecular sieves (1.043 g), and iron sulfate heptahydrate (0.146 g, 0.53 mmol) in methanol (5 mL). Purification: *n*-hexane/EtOAc/methanol/ $\text{NH}_3(\text{aq})$ (6/3.5/0.5/0.02, v/v/v/v) and then EtOAc/methanol (9/1, v/v). Yield: 51%; colorless oil. ^1H NMR (300 MHz, CDCl_3 , δ): 7.48 (dd, J = 2.1, 6.9 Hz, 1H), 7.33–7.26 (m, 1H), 7.22–7.14 (m, 1H), 6.83 (s, 4H), 4.50 (br s, 1H), 4.01 (t, J = 5.1 Hz, 2H), 3.76 (s, 3H), 3.60 (br s, 1H), 3.44–3.13 (m, 2H), 3.00 (t, J = 5.1 Hz, 2H), 2.90–2.78 (m, 2H), 2.02 (s, 2H), 1.64 (br s, 3H). ^{13}C NMR (75 MHz, CDCl_3 , δ): 168.1, 158.8 (d, J = 254 Hz), 154.0, 152.9, 132.9 (d, J = 4.4 Hz), 129.7, 127.1 (d, J = 7.7 Hz), 121.5 (d, J = 18.2 Hz), 116.8 (d, J = 22 Hz), 115.5 (2C), 114.7 (2C), 94.3 (d, J = 172 Hz), 68.0, 57.3 (d, J = 22 Hz), 55.7, 49.4, 43.8, 38.2, 33.8, 33.1. Formula: $\text{C}_{22}\text{H}_{25}\text{ClF}_2\text{N}_2\text{O}_3$; MS (ESI⁺) m/z : 439 [M + H⁺].

(3,4-Dichlorophenyl)(4-fluoro-4-(((2-(4-methoxyphenoxy)ethyl)amino)methyl)piperidin-1-yl)methanone (41). The title compound was prepared using 2-(1-(3,4-dichlorobenzoyl)-4-fluoropiperidin-4-yl)-2-hydroxyacetonitrile (5) (0.350 g, 1.06 mmol), 2-(4-methoxyphenoxy)ethanamine (14) (0.265 g, 1.59 mmol), DABCO (1.479 g, 13.18 mmol), sodium cyanoborohydride (0.518 g, 8.25 mmol), and molecular sieves (2.194 g) in methanol (10 mL). Purification: EtOAc/methanol (9/9/0.1, v/v). Yield: 30%; pale yellow crystallizing oil. ^1H NMR (300 MHz, CDCl_3 , δ): 7.54–7.44 (m, 2H), 7.23 (dd, J = 2.1, 8.2 Hz, 1H), 6.83 (s, 4H), 4.52 (br s, 1H), 4.01 (t, J = 5.1 Hz, 2H), 3.76 (s, 3H), 3.57 (br s, 1H), 3.45–3.10 (m, 2H), 3.00 (t, J = 5.0 Hz, 2H), 2.88–2.77 (m, 2H), 2.02 (m, 2H), 1.61 (br s, 3H). ^{19}F NMR (282 MHz, CDCl_3 , δ): –166.5 (s, 1F). ^{13}C NMR (75 MHz, CDCl_3 , δ): 167.9, 154.0, 152.9, 135.7, 134.1, 133.0, 130.6, 129.1, 126.2, 115.5 (2C), 114.6 (2C), 94.3 (d, J = 172 Hz), 68.0, 57.3 (d, J = 22 Hz), 55.7, 49.4, 43.6, 38.2, 33.5, 32.5. Formula: $\text{C}_{22}\text{H}_{25}\text{Cl}_2\text{FN}_2\text{O}_3$; MS (ESI⁺) m/z : 455 [M + H⁺].

2-((1-(3-Chloro-4-fluorobenzoyl)-4-fluoropiperidin-4-yl)methyl)aminoethoxybenzamide (42). The title compound was prepared using 2-(1-(3-chloro-4-fluorobenzoyl)-4-fluoropiperidin-4-yl)-2-hydroxyacetonitrile (4) (0.163 g, 0.52 mmol), 2-(2-aminoethoxy)benzamide (15) (0.140 g, 0.78 mmol), DABCO (0.725 g, 6.48 mmol), sodium cyanoborohydride (0.253 g, 4.04 mmol), molecular sieves (0.900 g), and iron sulfate heptahydrate (0.158 g, 0.57 mmol) in methanol (5 mL). Purification: *n*-hexane/Et₂O/DCM/methanol/ $\text{NH}_3(\text{aq})$ (3/2/4.5/0.5/0.02, v/v/v/v/v). Yield: 29%; white powder. ^1H NMR (300 MHz, $\text{DMSO}-d_6$, δ): 7.95 (s, 1H), 7.81 (dd, J = 1.8, 7.6 Hz, 1H), 7.65 (dd, J = 1.8, 7.0 Hz, 1H), 7.54 (br s, 1H), 7.50–7.37 (m, 3H), 7.12 (d, J = 8.2 Hz, 1H), 7.00 (t, J = 7.9 Hz, 1H), 4.33–4.07 (m, 3H), 3.38 (br s, 1H), 3.27–2.97 (m, 2H), 2.93 (t, J = 5.3 Hz, 2H), 2.81–2.66 (m, 2H), 2.13 (br s, 1H), 1.96–1.64 (m, 4H). ^{13}C NMR (75 MHz, $\text{DMSO}-d_6$, δ): 167.2, 166.7, 157.2, 158.1 (d, J = 248.7 Hz), 134.4, 132.9, 131.3, 129.7, 128.2 (d, J = 6.9 Hz), 123.1, 121.0, 120.2 (d, J = 18.3 Hz), 117.4 (d, J = 21 Hz), 113.8, 95.6 (d, J = 172 Hz), 68.5, 56.7 (d, J = 22 Hz), 49.0,

43.4, 38.0, 33.1, 32.3. Formula: $C_{22}H_{24}ClF_2N_3O_3$; MS (ESI⁺) m/z : 452 [M + H⁺]. mp 180.5–181.0 °C.

3-(2-(((1-(3-Chloro-4-fluorobenzoyl)-4-fluoropiperidin-4-yl)-methyl)amino)ethoxy)benzamide (43). The title compound was prepared using 2-(1-(3-chloro-4-fluorobenzoyl)-4-fluoropiperidin-4-yl)-2-hydroxyacetonitrile (4) (0.100 g, 0.32 mmol), 3-(2-aminoethoxy)benzamide (16) (0.080 g, 0.41 mmol), DABCO (0.444 g, 3.97 mmol), sodium cyanoborohydride (0.155 g, 2.48 mmol), molecular sieves (0.900 g), and iron sulfate heptahydrate (0.097 g, 0.35 mmol) in methanol (5 mL). Purification: EtOAc/methanol (9/1, v/v). Yield: 42%; yellow transparent oil. ¹H NMR (300 MHz, CDCl₃, δ): 7.46 (dd, $J = 1.8, 7.0$ Hz, 1H), 7.42–7.37 (m, 1H), 7.35–7.23 (m, 3H), 7.20–7.11 (m, 1H), 7.04 (td, $J = 2.9, 5.9$ Hz, 1H), 6.43–6.04 (m, 2H), 4.49 (br s, 1H), 4.09 (t, $J = 5.3$ Hz, 2H), 3.58 (br s, 1H), 3.45–3.08 (m, 2H), 3.02 (t, $J = 5.3$ Hz, 2H), 2.83 (d, $J = 19.9$ Hz, 2H), 1.98 (br s, 3H), 1.81–1.48 (m, 2H). ¹⁹F NMR (282 MHz, CDCl₃, δ): –112.6 (s, 1F), –166.4 (s, 1F). ¹³C NMR (75 MHz, CDCl₃, δ): 169.4, 168.1, 159.0, 158.8 (d, $J = 254$ Hz), 134.8, 132.8 (d, $J = 3.5$ Hz), 129.7, 129.6, 127.1 (d, $J = 7.7$ Hz), 121.5 (d, $J = 17.3$ Hz), 119.5, 118.6, 116.8 (d, $J = 22$ Hz), 113.3, 94.3 (d, $J = 172$ Hz), 67.5, 57.2 (d, $J = 22$ Hz), 49.1, 43.7, 38.3, 33.6, 32.8. Formula: $C_{22}H_{24}ClF_2N_3O_3$; MS (ESI⁺) m/z : 452 [M + H⁺].

(3-Chloro-4-fluorophenyl)(4-fluoro-4-(((2-(2-(methylamino)phenoxy)ethyl)amino)methyl)piperidin-1-yl)methanone (44). The title compound was prepared using 2-(1-(3-chloro-4-fluorobenzoyl)-4-fluoropiperidin-4-yl)-2-hydroxyacetonitrile (4) (0.120 g, 0.38 mmol), 2-(2-aminoethoxy)-*N*-methylaniline (24) (0.076 g, 0.46 mmol), DABCO (0.084 g, 0.76 mmol), sodium cyanoborohydride (0.038 g, 0.61 mmol), molecular sieves (0.900 g), and iron sulfate heptahydrate (0.117 g, 0.42 mmol) in methanol (5 mL). Purification: EtOAc/methanol (9.5/0.5, v/v). Yield: 29%; yellow transparent oil. ¹H NMR (300 MHz, CDCl₃, δ): 7.52–7.44 (m, 1H), 7.34–7.26 (m, 1H), 7.23–7.12 (m, 1H), 6.96–6.87 (m, 1H), 6.78 (dd, $J = 1.5, 7.9$ Hz, 1H), 6.64 (dq, $J = 1.8, 7.8$ Hz, 2H), 4.50 (br s, 1H), 4.09 (t, $J = 5.3$ Hz, 2H), 3.60 (br s, 1H), 3.45–3.13 (m, 2H), 3.05 (t, $J = 5.0$ Hz, 2H), 2.90–2.75 (m, 5H), 2.00 (br s, 3H), 1.64 (m, 3H). ¹⁹F NMR (282 MHz, CDCl₃, δ): –112.6 (s, 1F), –166.6 (s, 1F). ¹³C NMR (126 MHz, CDCl₃, δ): 168.2, 158.9 (d, $J = 252.3$ Hz), 145.9, 139.7, 132.9 (d, $J = 4.2$ Hz), 129.8, 127.2 (d, $J = 7.8$ Hz), 122.1, 121.7 (d, $J = 18.1$ Hz), 116.9 (d, $J = 21.1$ Hz), 116.4, 111.1, 109.8, 94.3 (d, $J = 172.6$ Hz), 67.6 (s), 57.1 (d, $J = 21.7$ Hz), 49.4, 43.6, 38.2, 33.6, 32.9, 30.4. Formula: $C_{22}H_{26}ClF_2N_3O_2$; MS (ESI⁺) m/z : 438 [M + H⁺].

(3-Chloro-4-fluorophenyl)(4-fluoro-4-(((2-(3-(methylamino)phenoxy)ethyl)amino)methyl)piperidin-1-yl)methanone (45). The title compound was prepared by Boc-deprotection of *tert*-butyl (3-(2-(((1-(3-chloro-4-fluorobenzoyl)-4-fluoropiperidin-4-yl)methyl)-amino)ethoxy)phenyl)(methyl)carbamate (27).

Compound 27 (1.0 equiv, 0.075 g, 0.14 mmol) was mixed with 1.0 M HCl in EtOAc (5 mL) and stirred at room temperature for 24 h. Then, the mixture was filtered to give the product as a hydrochloride salt. The obtained hydrochloride salt was turned into a free base (using 10% aqueous solution of sodium carbonate) before purification. Purification: DCM/methanol/NH₃(aq) (9.5/0.5/0.02, v/v/v). Yield: 48%; white-gray crystallizing oil. ¹H NMR (300 MHz, CD₃OD, δ): 7.73–7.00 (m, 7H), 4.46 (br s, 3H), 3.77–3.34 (m, 6H), 3.22 (br s, 1H), 3.08 (s, 3H), 2.19–1.81 (m, 4H), NH protons not detected. ¹⁹F NMR (282 MHz, CDCl₃, δ): –114.8 (s, 1F), –166.6 (s, 1F). ¹³C NMR (75 MHz, CDCl₃, δ): 169.0, 160.0 (d, $J = 3.5$ Hz), 156.1, 150.7 (d, $J = 4.7$ Hz), 129.7 (d, $J = 8.5$ Hz), 129.3, 128.8, 127.1, 122.5, 111.6, 105.9, 102.8, 98.9, 94.5 (d, $J = 172$ Hz), 67.0, 57.3 (d, $J = 22$ Hz), 56.2, 49.4, 43.9, 38.4, 33.7, 32.9. Formula: $C_{22}H_{26}ClF_2N_3O_2$; MS (ESI⁺) m/z : 438 [M + H⁺].

(3-Chloro-4-fluorophenyl)(4-(((2-(3-(dimethylamino)phenoxy)ethyl)amino)methyl)-4-fluoropiperidin-1-yl)methanone (46). The title compound was prepared using 2-(1-(3-chloro-4-fluorobenzoyl)-4-fluoropiperidin-4-yl)-2-hydroxyacetonitrile (4) (0.166 g, 0.53 mmol), 3-(2-aminoethoxy)-*N,N*-dimethylaniline (18) (0.133 g, 0.74 mmol), DABCO (0.740 g, 6.61 mmol), sodium cyanoborohydride (0.277 g, 4.13 mmol), molecular sieves (1.043 g), and iron sulfate heptahydrate (0.162 g, 0.58 mmol) in methanol (5 mL). Purification:

DCM/methanol/NH₃(aq) (9.5/0.5/0.02, v/v/v) and then *n*-hexane/EtOAc/methanol/NH₃(aq) (4/5.5/0.5/0.02, v/v/v/v). Yield: 42%; colorless oil. ¹H NMR (300 MHz, CDCl₃, δ): 7.48 (dd, $J = 2.1, 6.7$ Hz, 1H), 7.34–7.25 (m, 1H), 7.22–7.07 (m, 2H), 6.40–6.32 (m, 1H), 6.31–6.22 (m, 2H), 4.50 (br s, 1H), 4.06 (t, $J = 5.0$ Hz, 2H), 3.60 (br s, 1H), 3.47–3.08 (m, 2H), 3.02 (t, $J = 5.0$ Hz, 2H), 2.93 (s, 6H), 2.84 (d, $J = 19.9$ Hz, 2H), 2.00 (br s, 2H), 1.87–1.47 (m, 3H). ¹³C NMR (75 MHz, CDCl₃, δ): 168.0, 159.8, 158.8 (d, $J = 254$ Hz), 152.0, 132.9 (d, $J = 4.4$ Hz), 129.7 (d, $J = 2.3$ Hz, 2C), 127.1 (d, $J = 6.9$ Hz), 121.5 (d, $J = 18.4$ Hz), 116.8 (d, $J = 22$ Hz), 105.9, 101.9, 99.6, 94.4 (d, $J = 172$ Hz), 67.0, 57.3 (d, $J = 22$ Hz), 49.4, 43.7, 40.6 (2C), 38.1, 33.7, 32.9. Formula: $C_{23}H_{28}ClF_2N_3O_2$; MS (ESI⁺) m/z : 452 [M + H⁺].

***N*-(3-(2-(((1-(3-Chloro-4-fluorobenzoyl)-4-fluoropiperidin-4-yl)-methyl)amino)ethoxy)phenyl)acetamide (47)**. The title compound was prepared using 2-(1-(3-chloro-4-fluorobenzoyl)-4-fluoropiperidin-4-yl)-2-hydroxyacetonitrile (4) (0.150 g, 0.48 mmol), *N*-[3-(2-aminoethoxy)phenyl]acetamide (19) (0.148 g, 0.76 mmol), DABCO (0.669 g, 5.97 mmol), sodium cyanoborohydride (0.234 g, 3.73 mmol), molecular sieves (1.043 g), and iron sulfate heptahydrate (0.146 g, 0.53 mmol) in methanol (5 mL). Purification: EtOAc/methanol (9.5/0.5, v/v). Yield: 82%; colorless oil. ¹H NMR (500 MHz, CDCl₃, δ): 7.54 (br s, 1H), 7.47 (dd, $J = 1.9, 7.0$ Hz, 1H), 7.31–7.26 (m, 2H), 7.20–7.13 (m, 2H), 6.94 (br d, $J = 8.0$ Hz, 1H), 6.62 (br d, $J = 7.2$ Hz, 1H), 4.50 (br s, 1H), 4.13–4.06 (m, 2H), 3.59 (br s, 1H), 3.43–3.19 (m, 2H), 3.09 (br s, 2H), 2.93 (br d, $J = 19.8$ Hz, 2H), 2.14 (s, 3H), 2.11–1.91 (m, 3H), 1.83–1.58 (m, 2H). ¹³C NMR (75 MHz, CDCl₃, δ): 173.0, 168.7, 168.1, 159.2, 158.7 (d, $J = 254$ Hz), 139.4, 132.8 (d, $J = 4.4$ Hz), 129.6 (d, $J = 6.1$ Hz), 127.1 (d, $J = 7.7$ Hz), 121.5 (d, $J = 17.7$ Hz), 116.8 (d, $J = 22$ Hz), 112.2, 110.2, 106.4, 94.3 (d, $J = 172$ Hz), 67.3, 57.2 (d, $J = 22$ Hz), 49.2, 43.5, 38.1, 33.4, 32.5, 22.6. Formula: $C_{23}H_{26}ClF_2N_3O_3$; MS (ESI⁺) m/z : 466 [M + H⁺].

***N*-(3-(2-(((1-(3,4-Dichlorobenzoyl)-4-fluoropiperidin-4-yl)-methyl)amino)ethoxy)phenyl)acetamide (48)**. The title compound was prepared using 2-(1-(3,4-dichlorobenzoyl)-4-fluoropiperidin-4-yl)-2-hydroxyacetonitrile (5) (0.075 g, 0.23 mmol), *N*-[3-(2-aminoethoxy)phenyl]acetamide (19) (0.070 g, 0.36 mmol), DABCO (0.317 g, 2.83 mmol), sodium cyanoborohydride (0.111 g, 1.76 mmol), and molecular sieves (0.47 g) in methanol (3 mL). Purification: EtOAc/methanol (9/1 v/v). Yield: 18%; yellow oil. ¹H NMR (500 MHz, CDCl₃, δ): 7.66 (br s, 1H), 7.52–7.41 (m, 2H), 7.31 (br s, 1H), 7.21 (dd, $J = 1.7, 8.0$ Hz, 1H), 7.15 (br t, $J = 8.2$ Hz, 1H), 6.92 (br d, $J = 7.7$ Hz, 1H), 6.61 (br d, $J = 7.2$ Hz, 1H), 4.50 (br s, 1H), 4.06 (br t, $J = 4.9$ Hz, 2H), 3.56 (br s, 1H), 3.36 (br s, 1H), 3.12 (br s, 1H), 3.05 (br t, $J = 4.0$ Hz, 2H), 2.88 (br d, $J = 17.5$ Hz, 2H), 2.60 (br s, 1H), 2.13 (s, 3H), 2.08–1.88 (m, 2H), 1.66 (br s, 2H). ¹³C NMR (126 MHz, CDCl₃, δ): 168.5, 168.1, 159.4, 139.3, 135.7, 134.2, 133.1, 130.7, 129.7, 129.2, 126.3, 112.2, 110.4, 106.5, 94.4 (d, $J = 172.6$ Hz), 67.4, 57.3 (d, $J = 22.3$ Hz), 49.3, 43.7, 38.2, 33.7 (d, $J = 16.9$ Hz), 32.79 (d, $J = 17.5$ Hz), 24.8. Formula: $C_{23}H_{26}Cl_2FN_3O_3$; MS (ESI⁺) m/z : 482 [M + H⁺].

(3-Chloro-4-fluorophenyl)(4-fluoro-4-(((2-(*m*-tolylloxy)ethyl)amino)methyl)piperidin-1-yl)methanone (49). The title compound was prepared using 2-(1-(3-chloro-4-fluorobenzoyl)-4-fluoropiperidin-4-yl)-2-hydroxyacetonitrile (4) (0.120 g, 0.38 mmol), 2-(*m*-tolylloxy)ethanamine (20) (0.081 g, 0.54 mmol), DABCO (0.535 g, 4.78 mmol), sodium cyanoborohydride (0.178 g, 2.98 mmol), molecular sieves (0.900 g), and iron sulfate heptahydrate (0.117 g, 0.42 mmol) in methanol (5 mL). Purification: *n*-hexane/Et₂O/DCM/methanol/NH₃(aq) (3/2/4.5/0.5/0.02, v/v/v/v/v). Yield: 53%; white crystallizing oil. ¹H NMR (300 MHz, CD₃OD, δ): 7.59 (dd, $J = 1.8, 7.0$ Hz, 1H), 7.45–7.37 (m, 1H), 7.36–7.28 (m, 1H), 7.17–7.06 (m, 1H), 6.78–6.66 (m, 3H), 4.43 (br s, 1H), 4.05 (t, $J = 5.3$ Hz, 2H), 3.68–3.49 (m, 1H), 3.39 (br s, 1H), 3.28–3.09 (m, $J = 5.3$ Hz, 1H), 3.00 (t, $J = 5.6$ Hz, 2H), 2.91–2.79 (m, 2H), 2.29 (s, 3H), 2.06–1.62 (m, 4H), NH proton not detected. ¹³C NMR (75 MHz, CD₃OD, δ): 168.6, 158.8, 158.7 (d, $J = 251$ Hz), 139.2, 133.0 (d, $J = 4.6$ Hz), 129.3, 128.8, 127.3 (d, $J = 6.9$ Hz), 121.3, 120.9 (d, $J = 18.4$ Hz), 116.6 (d, $J = 21.8$ Hz), 114.9, 111.1, 93.8 (d, $J = 172.7$ Hz), 66.5, 56.5

(d, $J = 21.9$ Hz), 48.8, 43.6, 38.1, 32.9, 32.2, 20.2. Formula: $C_{22}H_{25}ClF_2N_2O_2$; MS (ESI⁺) m/z : 423 [M + H⁺].

(3-Chloro-4-fluorophenyl)(4-fluoro-4-((2-(3-(trifluoromethyl)phenoxy)ethyl)amino)methyl)piperidin-1-yl)methanone (**50**). The title compound was prepared using 2-(1-(3-chloro-4-fluorobenzoyl)-4-fluoropiperidin-4-yl)-2-hydroxyacetonitrile (**4**) (0.150 g, 0.48 mmol), 2-(3-(trifluoromethyl)phenoxy)ethanamine (**21**) (0.156 g, 0.76 mmol), DABCO (0.669 g, 5.97 mmol), sodium cyanoborohydride (0.234 g, 3.73 mmol), molecular sieves (1.043 g), and iron sulfate heptahydrate (0.146 g, 0.53 mmol) in methanol (5 mL). Purification: EtOAc/methanol (9.5/0.5, v/v) and then *n*-hexane/EtOAc (3/7, v/v). Yield: 49%; yellow transparent oil. ¹H NMR (300 MHz, CDCl₃, δ): 7.48 (dd, $J = 2.1$, 6.9 Hz, 1H), 7.42–7.34 (m, 1H), 7.33–7.26 (m, 1H), 7.24–7.16 (m, 2H), 7.13 (d, $J = 3.5$ Hz, 1H), 7.06 (dd, $J = 2.9$, 8.2 Hz, 1H), 4.48 (br s, 1H), 4.09 (t, $J = 5.0$ Hz, 2H), 3.75–3.48 (m, 1H), 3.47–3.10 (m, 2H), 3.05 (t, $J = 5.0$ Hz, 2H), 2.91–2.76 (m, 2H), 2.07–1.95 (m, 2H), 1.83–1.44 (m, 3H). ¹³C NMR (75 MHz, CDCl₃, δ): 168.1, 158.9, 158.8 (d, $J = 254$ Hz), 132.9 (d, $J = 4.6$ Hz), 131.8 (d, $J = 32.3$ Hz), 130.0, 129.7, 127.1 (d, $J = 8.1$ Hz), 123.9 (q, $J = 272$ Hz), 121.5 (d, $J = 18.2$ Hz), 117.9, 117.6 (q, $J = 3.9$ Hz), 116.8 (d, $J = 22$ Hz), 111.3 (q, $J = 3.9$ Hz), 94.3 (d, $J = 172$ Hz), 67.7, 57.3 (d, $J = 22$ Hz), 49.1, 43.5, 38.3, 33.7, 32.8. Formula: $C_{22}H_{22}ClF_2N_2O_2$; MS (ESI⁺) m/z : 477 [M + H⁺].

(3-Chloro-4-fluorophenyl)(4-fluoro-4-((2-(quinolin-8-yloxy)ethyl)amino)methyl)piperidin-1-yl)methanone (**51**). The title compound was prepared using 2-(1-(3-chloro-4-fluorobenzoyl)-4-fluoropiperidin-4-yl)-2-hydroxyacetonitrile (**4**) (0.200 g, 0.64 mmol), 2-(quinolin-8-yloxy)ethanamine (**25**) (0.192 g, 1.02 mmol), DABCO (0.892 g, 7.96 mmol), sodium cyanoborohydride (0.311 g, 4.99 mmol), molecular sieves (1.400 g), and iron sulfate heptahydrate (0.195 g, 0.70 mmol) in methanol (7 mL). Purification: EtOAc/methanol (9.5/0.5, v/v). Yield: 69%; beige crystallizing oil. ¹H NMR (300 MHz, CDCl₃, δ): 8.92 (dd, $J = 1.8$, 4.1 Hz, 1H), 8.15 (dd, $J = 1.7$, 8.3 Hz, 1H), 7.50–7.38 (m, 4H), 7.28 (dd, $J = 2.1$, 4.6 Hz, 1H), 7.19–7.12 (m, 1H), 7.09 (dd, $J = 1.7$, 7.3 Hz, 1H), 4.50 (br s, 1H), 4.34 (t, $J = 5.3$ Hz, 2H), 3.58 (br s, 1H), 3.39–3.13 (m, 4H), 2.98–2.86 (m, 2H), 2.06–1.97 (m, 2H), 1.66 (br s, 3H). ¹³C NMR (75 MHz, CDCl₃, δ): 168.0, 158.7 (d, $J = 254$ Hz), 154.5, 149.2, 140.2, 136.1, 132.9 (d, $J = 4.4$ Hz), 129.7, 129.5, 127.1 (d, $J = 7.2$ Hz), 126.7, 121.7, 121.4, 120.1, 116.7 (d, $J = 22$ Hz), 109.4, 94.3 (d, $J = 172$ Hz), 68.7, 57.3 (d, $J = 22$ Hz), 49.1, 43.6, 38.3, 33.6, 32.9. Formula: $C_{24}H_{24}ClF_2N_2O_2$; MS (ESI⁺) m/z : 460 [M + H⁺].

(3,4-Dichlorophenyl)(4-fluoro-4-((2-(quinolin-8-yloxy)ethyl)amino)methyl)piperidin-1-yl)methanone Fumarate Salt (**52**). The title compound was prepared using 2-(1-(3,4-dichlorobenzoyl)-4-fluoropiperidin-4-yl)-2-hydroxyacetonitrile (**5**) (0.597 g, 1.90 mmol), 2-(quinolin-8-yloxy)ethanamine (**25**) (0.395 g, 2.11 mmol), DABCO (2.660 g, 23.75 mmol), sodium cyanoborohydride (0.932 g, 14.82 mmol), and molecular sieves (3.200 g) in methanol (18 mL). Purification: EtOAc/methanol/NH₃(aq) (9.5/0.5/0.02, v/v/v). Yield: 15%; white oil. The compound was prepared as fumarate salt by adding a solution on fumaric acid in methanol (0.034 g in 2 mL methanol). ¹H NMR (500 MHz, CD₃OD, δ): 8.88 (dd, $J = 1.7$, 4.3 Hz, 1H), 8.37 (dd, $J = 1.6$, 8.4 Hz, 1H), 7.64–7.51 (m, 5H), 7.34 (dd, $J = 2.0$, 8.3 Hz, 1H), 7.27–7.22 (m, 1H), 6.66 (s, 2H), 4.53 (br s, 1H), 4.49 (t, $J = 4.8$ Hz, 2H), 3.68–3.54 (m, 3H), 3.50–3.37 (m, 3H), 3.20 (br s, 1H), 2.23–1.74 (m, 4H), NH protons not detected. ¹³C NMR (126 MHz, CD₃OD, δ): 169.6 (2C), 168.5, 152.9, 148.9, 138.8, 137.3, 135.6, 134.8 (2C), 133.9, 132.6, 130.8, 129.8, 128.9, 127.1, 126.4, 122.0, 120.6, 109.3, 91.8 (d, $J = 175.6$ Hz), 63.4, 53.9 (d, $J = 21.1$ Hz), 47.2, 42.9, 37.5, 32.5 (d, $J = 19.3$ Hz), 31.8 (d, $J = 26.6$ Hz). Formula: $C_{24}H_{24}Cl_2FN_2O_2 \cdot C_4H_4O_4$; MS (ESI⁺) m/z : 476 [M + H⁺].

(3-Chloro-4-fluorophenyl)(4-((2-(2,3-dihydrobenzo[b][1,4]-dioxin-5-yl)oxy)ethyl)amino)methyl)-4-fluoropiperidin-1-yl)methanone (**53**). The title compound was prepared using 2-(1-(3-chloro-4-fluorobenzoyl)-4-fluoropiperidin-4-yl)-2-hydroxyacetonitrile (**4**) (0.081 g, 0.26 mmol), 2-(2, 3-dihydro-1, 4-benzodioxin-6-yloxy)ethanamine (**22**) (0.080 g, 0.41 mmol), DABCO (0.359 g, 3.20 mmol), sodium cyanoborohydride (0.125 g, 2.00 mmol), and

molecular sieves (0.531 g) in methanol (3 mL). Purification: EtOAc/methanol (9.5/0.5, v/v). Yield: 19%, colorless oil. ¹H NMR (300 MHz, CDCl₃, δ): 7.48 (dd, $J = 2.1$, 6.9 Hz, 1H), 7.32–7.26 (m, 1H), 7.21–7.14 (m, 1H), 6.78–6.71 (m, 1H), 6.53 (ddd, $J = 1.3$, 8.2, 10.8 Hz, 2H), 4.50 (br s, 1H), 4.32–4.27 (m, 2H), 4.27–4.23 (m, 2H), 4.16–4.07 (m, 2H), 3.60 (br s, 1H), 3.34 (br s, 2H), 3.05 (t, $J = 5.3$ Hz, 2H), 2.91–2.78 (m, 2H), 2.02 (s, 2H), 1.63 (br s, 3H). Formula: $C_{23}H_{25}ClF_2N_2O_4$; MS (ESI⁺) m/z : 467 [M + H⁺].

(3,4-Dichlorophenyl)(4-((2-(2,3-dihydrobenzo[b][1,4]-dioxin-5-yl)oxy)ethyl)amino)methyl)-4-fluoropiperidin-1-yl)methanone (**54**). The title compound was prepared using 2-(1-(3,4-chlorobenzoyl)-4-fluoropiperidin-4-yl)-2-hydroxyacetonitrile (**5**) (0.200 g, 0.60 mmol), 2-(2,3-dihydro-1,4-benzodioxin-6-yloxy)ethanamine (**22**) (0.189 g, 0.97 mmol), DABCO (0.847 g, 7.55 mmol), sodium cyanoborohydride (0.296 g, 4.71 mmol), and molecular sieves (1.254 g) in methanol (6 mL). Purification: EtOAc/methanol (9.9/0.1, v/v) and then *n*-hexane/EtOAc/methanol/NH₃(aq) (4/5.5/0.5/0.02, v/v/v). Yield: 30%; pale yellow oil. ¹H NMR (300 MHz, CDCl₃, δ): 7.53–7.46 (m, 2H), 7.23 (dd, $J = 1.8$, 8.2 Hz, 1H), 6.78–6.71 (m, 1H), 6.52 (ddd, $J = 1.4$, 8.3, 10.8 Hz, 2H), 4.51 (br s, 1H), 4.31–4.27 (m, 2H), 4.27–4.23 (m, 2H), 4.11 (t, $J = 5.4$ Hz, 2H), 3.56 (br s, 1H), 3.45–3.11 (m, 2H), 3.04 (t, $J = 5.1$ Hz, 2H), 2.90–2.79 (m, 2H), 2.08–1.92 (m, 2H), 1.67 (br s, 3H). ¹⁹F NMR (282 MHz, CDCl₃, δ): –166.3 (s, 1F). ¹³C NMR (75 MHz, CDCl₃, δ): 167.9, 148.2, 144.4, 135.7, 134.1, 133.9, 133.0, 130.6, 129.1, 126.2, 120.2, 110.5, 106.3, 95.5 (d, $J = 172$ Hz), 69.0, 64.4, 64.2, 57.3 (d, $J = 22$ Hz), 49.2, 43.5, 39.0, 33.6, 32.6. Formula: $C_{23}H_{25}Cl_2FN_2O_4$; MS (ESI⁺) m/z : 483 [M + H⁺].

(3-Chloro-4-fluorophenyl)(4-((2-(2-dimethyl-2,3-dihydrobenzofuran-7-yl)oxy)ethyl)amino)methyl)-4-fluoropiperidin-1-yl)methanone (**55**). The title compound was prepared using 2-(1-(3-chloro-4-fluorobenzoyl)-4-fluoropiperidin-4-yl)-2-hydroxyacetonitrile (**4**) (0.100 g, 0.32 mmol), 2-(2-(2-dimethyl-2,3-dihydrobenzofuran-7-yl)oxy)ethanamine (**23**) (0.092 g, 0.45 mmol), DABCO (0.444 g, 3.97 mmol), sodium cyanoborohydride (0.155 g, 2.48 mmol), molecular sieves (0.900 g), and iron sulfate heptahydrate (0.097 g, 0.35 mmol) in methanol (5 mL). Purification: *n*-hexane/DCM/methanol/NH₃(aq) (4/5.5/0.5/0.02, v/v/v/v). Yield: 33%; yellow oil. ¹H NMR (300 MHz, CDCl₃, δ): 7.48 (dd, $J = 1.8$, 7.0 Hz, 1H), 7.32–7.25 (m, 1H), 7.22–7.13 (m, 1H), 6.81–6.70 (m, 3H), 4.50 (br s, 1H), 4.15 (t, $J = 5.0$ Hz, 2H), 3.71–3.50 (m, 1H), 3.48–3.08 (m, 2H), 3.06–2.96 (m, 4H), 2.83 (d, $J = 19.9$ Hz, 2H), 1.99 (br s, 2H), 1.83 (br s, 3H), 1.49 (s, 6H). ¹³C NMR (75 MHz, CDCl₃, δ): 168.0, 158.8 (d, $J = 254$ Hz), 147.9, 143.5, 132.9 (d, $J = 3.5$ Hz), 129.7, 128.6, 127.1 (d, $J = 8.1$ Hz), 121.5 (d, $J = 18.4$ Hz), 120.3, 118.1, 116.8 (d, $J = 22$ Hz), 113.7, 94.3 (d, $J = 172$ Hz), 87.3, 69.0, 57.2 (d, $J = 22$ Hz), 49.2, 43.6, 43.2, 38.3, 33.5, 32.8, 28.3 (2C). Formula: $C_{25}H_{29}ClF_2N_2O_3$; MS (ESI⁺) m/z : 479 [M + H⁺].

(4-((2-(1*H*-indol-4-yl)oxy)ethyl)amino)methyl)-4-fluoropiperidin-1-yl)(3-chloro-4-fluorophenyl)methanone Fumarate Salt (**56**). The title compound was prepared using 2-(1-(3-chloro-4-fluorobenzoyl)-4-fluoropiperidin-4-yl)-2-hydroxyacetonitrile (**4**) (0.150 g, 0.48 mmol), 2-(1*H*-indol-4-yl)oxyethanamine (**26**) (0.126 g, 0.72 mmol), DABCO (0.669 g, 5.97 mmol), sodium cyanoborohydride (0.234 g, 3.73 mmol), molecular sieves (1.043 g), and iron sulfate heptahydrate (0.146 g, 0.53 mmol) in methanol (5 mL). Purification: *n*-hexane/EtOAc/methanol/NH₃(aq) (3/6.5/0.5/0.02, v/v/v/v). Yield: 64%; beige powder. The compound was prepared as fumarate salt by adding a solution on fumaric acid in methanol (0.035 g in 2 mL methanol). ¹H NMR (500 MHz, CD₃OD, δ): 7.58 (dd, $J = 2.0$, 7.2 Hz, 1H), 7.40–7.35 (m, 1H), 7.35–7.30 (m, 1H), 7.14 (d, $J = 3.2$ Hz, 1H), 7.08–6.99 (m, 2H), 6.71 (s, 2H), 6.58 (d, $J = 2.9$ Hz, 1H), 6.54 (d, $J = 7.4$ Hz, 1H), 4.49 (br s, 1H), 4.43 (t, $J = 5.2$ Hz, 2H), 3.60 (br s, 1H), 3.56 (t, $J = 5.0$ Hz, 2H), 3.48–3.35 (m, 3H), 3.19 (br s, 1H), 2.09 (br s, 1H), 1.98 (s, 2H), 1.91–1.72 (m, 2H), NH protons not detected. ¹³C NMR (126 MHz, CD₃OD, δ): 170.0 (2C), 169.6, 159.8 (d, $J = 251.1$ Hz), 152.2, 138.9, 135.5 (2C), 133.7 (d, $J = 4.2$ Hz), 130.4, 128.3 (d, $J = 7.8$ Hz), 123.9, 122.5, 121.9 (d, $J = 18.1$ Hz), 119.6, 117.7 (d, $J = 22.3$ Hz), 106.4, 100.9, 99.1, 92.9 (d, $J = 175.0$

Hz), 64.1, 55.1 (d, $J = 20.5$ Hz), 48.9, 43.9, 38.5, 33.3, 32.6. Formula: $C_{23}H_{24}ClF_2N_3O_2 \cdot C_4H_4O_4$; MS (ESI⁺) m/z : 448 [M + H⁺].

(3-Chloro-4-fluorophenyl)(4-fluoro-4-((2-(indolin-4-yl)oxy)ethyl)amino)methyl)piperidin-1-yl)methanone (57). The title compound was prepared by the reduction of ((4-((2-((1H-indol-4-yl)oxy)ethyl)amino)methyl)-4-fluoropiperidin-1-yl)(3-chloro-4-fluorophenyl)methanone) (56).

To a solution of compound 56 (1.0 equiv, 0.177 g, 0.40 mmol) in acetic acid (1.0 equiv, 0.23 mL, 0.40 mmol) sodium cyanoborohydride (2.0 equiv 0.051 g, 0.80 mmol) was added in portions at 15 °C. Then, the mixture was warmed up to room temperature and stirred for an hour. The reaction mixture was then cooled to 0 °C, quenched, and adjusted to pH 8 with a saturated aqueous solution of sodium bicarbonate and extracted with EtOAc (3 \times). The organic layers were combined and dried over magnesium sulfate, filtered, and concentrated to yield the crude product that was purified by flash chromatography in *n*-hexane/EtOAc/methanol/NH_{3(aq)} (6/3/1/0.02, v/v/v/v). Yield: 67%; pale pink transparent oil. ¹H NMR (300 MHz, CDCl₃, δ): 7.48 (dd, $J = 2.3, 7.0$ Hz, 1H), 7.35–7.26 (m, 1H), 7.23–7.11 (m, 1H), 6.97 (t, $J = 7.9$ Hz, 1H), 6.29 (dd, $J = 7.9, 14.4$ Hz, 2H), 4.51 (br s, 1H), 4.08 (t, $J = 5.0$ Hz, 2H), 3.56 (t, $J = 8.5$ Hz, 3H), 3.47–3.08 (m, 2H), 3.06–2.93 (m, 4H), 2.91–2.76 (m, 2H), 2.02 (br s, 2H), 1.85–1.44 (m, 2H), NH protons not detected. ¹⁹F NMR (282 MHz, CDCl₃, δ): –112.6 (s, 1F), –166.7 (s, 1F). ¹³C NMR (75 MHz, CDCl₃, δ): 168.0, 158.8 (d, $J = 254$ Hz), 155.6, 153.5, 132.9 (d, $J = 3.5$ Hz), 129.7, 128.6, 127.1 (d, $J = 6.9$ Hz), 121.5 (d, $J = 18$ Hz), 116.8 (d, $J = 22$ Hz), 116.0, 103.3, 102.6, 94.4 (d, $J = 172$ Hz), 67.2, 57.2 (d, $J = 22$ Hz), 49.3, 47.4, 43.5, 38.2, 33.5, 32.7, 26.9. Formula: $C_{23}H_{26}ClF_2N_3O_2$; MS (ESI⁺) m/z : 450 [M + H⁺].

In Vitro Studies. The tested compounds were examined for known classes of assay interference compounds. None of the compounds contain substructural features recognized as pan assay interference compounds (PAINS), according to the SwissADME tool.³²

Radioligand Binding Assays for 5-HT_{1A}R, α_1 R, D₂R. Preparation of Solutions of Test and Reference Compounds. Stock solutions (1 mM) of tested compounds were prepared in DMSO. Serial dilutions of compounds were prepared in a 96-well microplate in assay buffers using automated pipetting system epMotion 5070 (Eppendorf). The final concentration of DMSO in the test solutions was 0.1%. Each compound was tested in 10 concentrations from 1.0×10^{-6} to 1.0×10^{-12} M (final concentration).

Serotonin 5-HT_{1A} Receptor Binding Assay. Radioligand binding was performed using membranes from CHO-K1 cells stably transfected with the human 5-HT_{1A} receptor (PerkinElmer). All assays were carried out in duplicate. A working solution (50 μ L) of the tested compounds, 50 μ L of [³H]-8-OH-DPAT (final concentration 1 nM), and 150 μ L of diluted membranes (10 μ g protein per well) prepared in assay buffer (50 mM Tris, pH 7.4, 10 mM MgSO₄, 0, 5 mM EDTA, 0.1% ascorbic acid) were transferred to a polypropylene 96-well microplate using a 96-well pipetting station Rainin Liquidator (MettlerToledo). Serotonin (10 μ M) was used to define nonspecific binding. The microplate was covered with a sealing tape, mixed, and incubated for 60 min at 27 °C. The reaction was terminated by rapid filtration through a GF/C filter mate presoaked with 0.3% polyethyleneimine for 30 min. Ten rapid washes with 200 μ L 50 mM Tris buffer (4 °C, pH 7.4) were performed using an automated harvester system Harvester-96 MACH III FM (Tomtec). The filter mates were dried at 37 °C in forced air fan incubator and then solid scintillator MeltiLex was melted on filter mates at 90 °C for 4 min. Radioactivity was counted in MicroBeta2 scintillation counter (PerkinElmer). Data were fitted to a one-site curve-fitting equation with Prism 6 (GraphPad Software) and K_i values were estimated from the Cheng–Prusoff equation.

Adrenergic α_1 Receptor Binding Assay. Radioligand binding was performed using rat cortex. Tissue was homogenized in 20 volumes of ice-cold 50 mM Tris-HCl buffer, pH 7.6, using an Ultra Turrax T25B (IKA) homogenizer. The homogenate was centrifuged at 20,000g for 20 min. The resulting supernatant was decanted and the pellet was

resuspended in the same buffer and centrifuged again in the same conditions. The final pellet was resuspended in an appropriate volume of buffer (10 mg/1 mL). All assays were carried out in duplicate. The working solution (50 μ L) of the tested compounds, 50 μ L of [³H]-prazosin (final concentration 0.2 nM), and 150 μ L of tissue suspension were transferred to a polypropylene 96-well microplate using a 96-well pipetting station Rainin Liquidator (MettlerToledo). Phentolamine (10 μ M) was used to define nonspecific binding. The microplate was covered with a sealing tape and the content mixed and incubated for 30 min at 30 °C. The incubation was terminated by rapid filtration over glass fiber filters FilterMate B (PerkinElmer, USA) using a 96-well FilterMate harvester (PerkinElmer, USA). Five rapid washes were performed with ice-cold 50 mM Tris-HCl buffer, pH 7.6. The filter mates were dried at 37 °C in a forced air fan incubator and then solid scintillator MeltiLex was melted on filter mates at 90 °C for 5 min. Radioactivity was counted in a MicroBeta2 scintillation counter (PerkinElmer). Data were fitted to a one-site curve-fitting equation with Prism 6 (GraphPad Software) and K_i values were estimated from the Cheng–Prusoff equation.

Dopamine D₂ Receptor Binding Assay. Radioligand binding was performed using membranes from CHO-K1 cells stably transfected with the human D₂ receptor (PerkinElmer). All assays were carried out in duplicate. A working solution (50 μ L) of the tested compounds, 50 μ L of [³H]-methylspiperone (final concentration 0.4 nM), and 150 μ L of diluted membranes (3 μ g protein per well) prepared in assay buffer (50 mM Tris, pH 7.4, 50 mM HEPES, 50 mM NaCl, 5 mM MgCl₂, 0.5 mM EDTA) were transferred to a polypropylene 96-well microplate using a 96-well pipetting station Rainin Liquidator (MettlerToledo). Haloperidol (10 μ M) was used to define nonspecific binding. The microplate was covered with a sealing tape, and the mixture was mixed and incubated for 60 min at 37 °C. The reaction was terminated by rapid filtration through a GF/B filter mate presoaked with 0.5% polyethyleneimine for 30 min. Ten rapid washes with 200 μ L of 50 mM Tris buffer (4 °C, pH 7.4) were performed using an automated harvester system Harvester-96 MACH III FM (Tomtec). The filter mates were dried at 37 °C in a forced air fan incubator and then solid scintillator MeltiLex was melted on filter mates at 90 °C for 5 min. Radioactivity was counted in a MicroBeta2 scintillation counter (PerkinElmer). Data were fitted to a one-site curve-fitting equation with Prism 6 (GraphPad Software) and K_i values were estimated from the Cheng–Prusoff equation.

Functional Assays for the 5-HT_{1A} Receptor. ERK1/2 Phosphorylation. Test and reference compounds were dissolved in dimethyl sulfoxide (DMSO) at a concentration of 10 mM. Serial dilutions were prepared in a 96-well microplate in HBSS with 0.1% BSA added and eight concentrations were tested. The final concentration of DMSO in the test solutions was 0.1%.

The CHO-SHT_{1A} receptor cells were tested for agonist-induced ERK1/2-phosphorylation using the SureFire ERK1/2-phosphorylation α LISA assay kit according to the manufacturer's instruction (Perkin Elmer). After thawing, cells were cultured in medium [advanced DMEM/F12 with 1% fetal bovine serum (FBS) dialyzed, 400 μ g/mL G-418, 4 mM L-glutamine]. At the experiment, cells were plated at 50,000 cells/well of a 96-well tissue culture plate and grown 7 h in an incubator (5% CO₂, 37 °C); after this time, the cells were starving (DMEM/F12 with 0, 1% BSA (immunoglobulin- and protease-free) for 12 h. The serial dilutions of compounds were added and incubated for 15 min in 37 °C. The medium was removed, "lysis buffer" (70 μ L) was added and the plate gently agitated on a plate shaker (10 min). The plates were frozen at –80 °C. The next day, the plate was thawed on plate shaker for 10 min and 10 μ L was transferred to assay plates (384-OptiPlate, Perkin Elmer) in duplicate and 10 μ L of the reaction mix α LISA SureFire Ultra assay (Perkin Elmer) was added. The plate was incubated for 2 h at 22 °C. After incubation, the assay plate was measured in an EnVision multi-function plate reader (PerkinElmer Life Science). E_{max} values were defined as the response of the ligand expressed as a percentage of the maximal response elicited by serotonin, determined by nonlinear regression using GraphPad Prism 6.0 software. pEC₅₀ values

correspond to the ligand concentration at which 50% of its own maximal response was measured.

cAMP Inhibition. Tested and reference compounds were dissolved in DMSO to the concentration of 10 mM. Dilutions were prepared in a 96-well microplate in assay buffers. For 5-HT_{1A} receptors, adenylyl cyclase activity was determined using cryopreserved CHO-K1 cells with expression of the human serotonin 5-HT_{1A} receptor. The final concentration of DMSO in the test solutions was 0.1%.

The functional assay was performed with the CHO-K1 cells with expression of the 5-HT_{1A} human serotonin receptor in which plasmid containing the coding sequence was transfected. The cells were cultured under selective conditions (400 µg/mL Geneticin G418) (PerkinElmer). Thawed cells were resuspended in stimulation buffer (HBSS, 5 mM HEPES, 0.5 IBMX, and 0.1% BSA at pH 7.4) at 2×10^5 cells/mL. The same volume (10 µL) of cell suspension was added to tested compounds with 10 µM forskolin. Samples were loaded onto a white opaque half-area 96-well microplate. Cell stimulation was performed for 40 min at room temperature. After incubation, cAMP measurements were performed with homogeneous time-resolved fluorescence resonance energy transfer (TR-FRET) immunoassay using the LANCE Ultra cAMP kit (PerkinElmer, USA). Ten microliters of EucAMP Tracer Working Solution and 10 µL of ULight-anti-cAMP Tracer Working Solution were added, mixed, and incubated for 1 h. The TR-FRET signal was read on an EnVision microplate reader (PerkinElmer, USA). E_{\max} values were defined as the response of the ligand expressed as a percentage of the maximal response elicited by serotonin, determined by nonlinear regression using GraphPad Prism 6.0 software. pEC_{50} values correspond to the ligand concentration at which 50% of its own maximal response was measured.

β-Arrestin Recruitment. Test and reference compounds were dissolved in DMSO at a concentration of 10 mM. Serial dilutions were prepared in 96-well microplate in Dulbecco's modified Eagle's medium (DMEM) with 10% FBS added and eight concentrations were tested. The final concentration of DMSO in the test solutions was 0.1%.

The HTR1A-bla U2OS receptor cells containing the human Serotonin Type 1A receptor linked to a TEV protease site and a Gal4-VP16 transcription factor were tested for agonist induced using the Tango LiveBLazer assay kit according to the manufacturer's instruction (Life Technologies). After thawing, cells were cultured in medium (McCoy's 5A with 10% FBS dialyzed, 0.1 mM NEAA, 25 mM HEPES, 1 mM sodium pyruvate, 100 µg/mL G-418, 100 U/mL penicillin/streptomycin antibiotic, 200 µg/mL zeocin, 50 µg/mL hygromycin). At the experiment, cells were plated at 10,000 cells/well of a 384-well black, clear bottom, tissue culture plate and grown for 12 h in an incubator (5% CO₂, 37 °C) in DMEM with 10% FBS added. The serial dilutions of compounds were added and incubated for 5 h (5% CO₂, 37 °C). After this time, 8 µL of reaction mix was added. The plate was incubated for 2 h at 22 °C. After incubation, the assay plate was measured in a FLUOstar Optima multifunction plate reader (PerkinElmer Life Science). E_{\max} values were defined as the response of the ligand expressed as a percentage of the maximal response elicited by serotonin, determined by nonlinear regression using GraphPad Prism 6.0 software. pEC_{50} values correspond to the ligand concentration at which 50% of its own maximal response was measured.

Calcium Mobilization Assay. Test and reference compounds were dissolved in DMSO at a concentration of 10 mM. Serial dilutions were prepared in a 96-well microplate in assay buffer and 8–10 concentrations were tested. The final concentration of DMSO in the test solutions was 0.1%.

A cellular aequorin-based functional assay was performed with recombinant CHO-K1 cells expressing mitochondrially targeted aequorin, human GPCR and the promiscuous G protein α_{16} for 5-HT_{1A} receptor. Assay was executed according to a previously described protocol. After thawing, cells were transferred to assay buffer (DMEM/HAM's F12 with 0.1% protease free BSA) and centrifuged. The cell pellet was resuspended in assay buffer and coelenterazine h was added at a final concentration of 5 µM. The cell

suspension was incubated at 16 °C, protected from light with constant agitation for 16 h, and then diluted with assay buffer to the concentration of 100,000 cells/mL. After 1 h of incubation, 50 µL of the cell suspension was dispensed using automatic injectors built into the radiometric and luminescence plate counter MicroBeta2 LumijET (PerkinElmer, USA) into white opaque 96-well microplates preloaded with test compounds. Immediate light emission generated following calcium mobilization was recorded for 30 s. In antagonist mode, after 25 min of incubation, the reference agonist was added to the above assay mix and light emission was recorded again. The final concentration of the reference agonist was equal to EC₈₀ (300 nM serotonin).

Developability Studies. Preliminary Metabolic Stability Assessment. The *in vitro* evaluation of metabolic stability of phenoxyethyl derivatives of 1-(1-benzoyl-4-fluoropiperidin-4-yl)methanamine was performed by using RLMs (Sigma-Aldrich, St. Louis, MO, USA) according to previously described methods and protocols.^{53–55} The reaction mixtures were prepared first, consisting of 50 µM of the tested compound, microsomes (1 mg/mL), and 10 mM Tris-HCl buffer, pH = 7.4. Reaction mixtures were preliminarily incubated for 5 min in a temperature of 37 °C. After preincubation, 50 µL of an NADPH Regeneration System (Promega, Madison, WI, USA) was added to initiate the reaction. The reaction mixtures were incubated for 2 h at a temperature of 37 °C. In order to terminate the reaction, 200 µL of cold extrapure methanol was added. Then, the mixtures were centrifuged (14,000 rpm, 15 min) and the supernatants were analyzed using an LC/MS Waters ACQUITY TQD system with the TQ Detector (Waters, Milford, USA).

In silico prediction of metabolic biotransformations was performed by MetaSite 6.0.1 software (Molecular Discovery Ltd, Hertfordshire, UK).⁵⁶ The computational liver model of metabolism was used for determination of the most probable sites of metabolism and identification of structures of obtained *in vitro* metabolites.

Intrinsic Clearance. For determination of the intrinsic clearance (CL_{int}) parameter, five independent reactions were terminated by the addition of cold methanol containing IS at different time points: 0, 5, 15, 30, 45 min. The reaction mixtures were next centrifuged at 14,500 rpm for 10 min. The course of reaction was followed by using the analyte/IS peak height ratio values. In the determination of the *in vitro* $t_{1/2}$ value, the slope of linear regression from log concentration remaining versus time relationships ($-k$) was used according to Obach (1999). The supernatants with 3, 44, and 56 were analyzed by an HPLC system (LaChrom Elite, Merck-Hitachi, Germany) consisting of an L-2130 pump, an L-2200 autosampler, and an L-2420 UV-VIS detector. EZChrome Elite v. 3.2 (Merck-Hitachi, Germany) computer program was used for data acquisition and integration. The separation of studied compounds was performed using a 250 × 4.6 mm Supelcosil LC-CN column with a particle size of 5 µm (Sigma-Aldrich, Germany) protected with a guard column (20 × 4 mm) with the same packing material. The mobile phase consisted of 50 mM potassium dihydrogen phosphate (pH = 4.6), methanol, and acetonitrile mixed at a ratio of 51:40:9 v/v/v and run at 1 mL/min. Chromatographic analysis was carried out at 25 °C and the analytical wavelength was 205 nm.

PAMPA Assay. The ability to passive transport across a cell membrane was determined by precoated PAMPA Plate System Gentest (Corning, Tewksbury, MA, USA) according to described previously protocols.^{54,55} The compounds' concentrations in acceptor and donor wells were estimated by the UPLC-MS analyses, which were performed by LC/MS Waters ACQUITY TQD system with the TQ Detector (Waters, Milford, USA). The permeability coefficients (Pe, cm/s) were calculated according described previously formulas.⁵⁷

The substrates of Pgp were determined by the luminescent Pgp-Glo Assay System (Promega, Madison, WI, USA). The test measures luminescently the ATP consuming by Pgp in the presence of substrates. The assay was performed in triplicate as described previously.⁵⁵ Tested compounds (100 µM) were incubated with Pgp membranes for 40 min at 37 °C. The positive (VL) and negative (CFN) controls were incubated at 200 and 100 µM, respectively. Basal activity of Pgp was considered as the difference in the

luminescent signal between samples treated with 100 μM of the potent and selective Pgp inhibitor (Na_3VO_4) and untreated samples. The luminescence signal was measured by microplate reader EnSpire PerkinElmer (Waltham, MA, USA). Caffeine (CFN) and norfloxacin were purchased from Sigma-Aldrich (St. Louis, MO, USA).

Hepatotoxicity. The hepatotoxicity was investigated with use of a hepatoma HepG2 (ATCC HB-8065) cell line. Cells were grown under described previously conditions.⁵⁴ The cells viability was determined by CellTiter 96 Aqueous Non-Radioactive Cell Proliferation Assay (Promega, Madison, WI, USA) after 72 h of incubation with tested compounds at a final concentration range (0.1–100 μM). The reference toxins CCCP and doxorubicin (DX) were used at 10 and 1 μM , respectively. The absorbance was measured using a microplate reader EnSpire (PerkinElmer, Waltham, MA USA) at 490 nm. The compounds and references were tested in quadruplicate. DX was purchased from Sigma-Aldrich (St. Louis, MO, USA).

Extended Selectivity Studies. The off-target receptor screen and cardiac toxicity (hERG automated patch-clamp method) assays were performed by Eurofins Pharma Discovery Services according to well-known methods. Further methodological details are available on the company web site (www.eurofinsdiscoveryservices.com) and the appropriate publications.^{58–65}

In Vivo Pharmacodynamics Studies. Animals. The experiments were performed on male Wistar rats (170–200 g) obtained from an accredited animal facility at the Jagiellonian University Medical College, Krakow, Poland. The animals were housed in groups of four in a controlled environment (ambient temperature 21 ± 2 °C; relative humidity 50–60%; 12 h light/dark cycles (lights on at 8:00). Standard laboratory food (LSM-B) and filtered water were freely available. Animals were housed for a period of 6 days in polycarbonate Makrolon type 3 cages (dimensions $26.5 \times 15 \times 42$ cm, “open top”) without enrichment environment (only wooden shavings litter). Each animal was assigned randomly to treatment groups and only used once (no repeated use of animals). All the experiments were performed by two observers unaware of the treatment applied between 9:00 and 14:00 on separate groups of animals. All experimental procedures involving animals were conducted in accordance with European Union (Directive 2010/63/EU) and Polish legislation acts concerning animal experimentation and approved by the II Local Ethics Committee for Experiments on Animals in Cracow, Poland (approval number: 108/2016). All efforts were made to minimize suffering and to reduce the number of animals used in the experiments and to use only the number of animals necessary to produce reliable scientific data. Each experimental group consisted of 6–8 animals.

Drugs. All drugs were dissolved in distilled water immediately before administration in a volume of 2 mL/kg. The examined compounds were administered orally 60 min before tests. In antagonism experiments, WAY100635 (Tocris, UK) was administered subcutaneously 75 min before testing. Control animals received vehicle (distilled water) according to the same schedule.

Porsolt FST. The experiment was carried out according to the method of Porsolt *et al.*⁶⁶ On the first day of an experiment, the animals were individually gently placed in plexiglas cylinders (40 cm high, 18 cm in diameter) containing 17 cm of water maintained at 23–25 °C for 15 min. On removal from water, the rats were placed for 30 min in a plexiglas box under a 60 W bulb to dry. On the following day (24 h later), the rats were re-placed in the cylinder after administration of test compounds and the total duration of immobility was recorded during the 5-min test period. Immobility was considered to occur when no additional activity was observed other than that necessary to keep the rat's head above the water.⁶⁷ Fresh water was used for each animal.

Lower Lip Retraction. Observations were made according to the method described by Kleven *et al.*⁶⁸ Animals were observed individually during a 10 min period for 10 s of observation per animal. During each of these observation periods, the uninterrupted presence for at least 3 s (1) or absence (0) of LLR was recorded. This

cycle was repeated 10 times over a 10 min period; thus, the incidence of a particular behavior could vary from 0 to 10.

Statistical Analysis. The data of behavioral studies were evaluated by an analysis of variance: one-way ANOVA (when one drug was given) or two-way ANOVA (when two drugs were used) followed by Bonferroni's post hoc test (statistical significance set at $p < 0.05$).

In Vivo Pharmacokinetics Studies. Animals. Male Wistar rats weighing 200–250 g were used in this study. The investigated compounds were dissolved in water and administered orally at three different doses, that is, 0.31, 0.63, and 1.25 mg/kg (**56**) and 0.04, 0.16, 0.63 mg/kg (**44**). One hour following compound administration, the animals were sacrificed by decapitation and blood and brains were harvested. The blood was allowed to clot at room temperature and subsequently centrifuged at 3000 rpm for 10 min (Universal 32 centrifuge, Hettich, Germany) to obtain serum. All collected samples were frozen at -80 °C until assayed.

Determination of 56 and 44 in Serum and Brain Tissue. Serum and brain concentrations of the studied compounds were measured by HPLC with UV detection. The brains were homogenized in distilled water (1:4, w/v) with a tissue homogenizer TH220 (Omni International, Inc., Warrenton, VA, USA). The extraction of both compounds from serum and brain homogenates was performed using a mixture of ethyl acetate and hexane (30:70, v/v). The IS for **56** was 6-[[{[1-(3-chloro-4-fluorobenzoyl)-4-fluoropiperidin-4-yl]methyl}amino)methyl]-N,3-dimethylpyridin-2-amine (0.5 $\mu\text{g}/\text{mL}$ for serum samples and 2 $\mu\text{g}/\text{mL}$ for brain homogenates) and for **44** it was (3-chloro-4-fluorophenyl)(4-fluoro-4-(((5-methylpyridin-2-yl)methyl)amino)methyl)piperidin-1-yl)methanone (2 $\mu\text{g}/\text{mL}$ for both serum and brain samples) as methanolic solutions.

To isolate **56** and **44** from serum (1.5 mL) or brain homogenate (2 mL) containing these compounds, an appropriate IS (10 μL) was added and the samples were alkalized with 100 μL of 4 M NaOH. Then, the samples were extracted with 6 mL of the extraction reagent by shaking for 20 min (IKA Vibrax VXR, Germany). After centrifugation at 3000 rpm for 20 min (Universal 32, Hettich, Germany), the organic layers were transferred to new tubes containing 150 μL solution of 0.1 M H_2SO_4 and methanol (90:10 v/v). The mixtures were shaken for 20 min and centrifuged for 20 min (3000 rpm). The organic layer was discarded and 60–80 μL aliquots of the acidic solutions were injected into the HPLC system.

The analytical procedure for ultrafiltrate was similar to that described above, with the exception that 300 μL of this matrix was used for analysis, the volumes of 4 M NaOH and the extraction solvent were 20 μL and 1 mL, respectively, and the organic layers were transferred to 100 μL of the acidic solution.

The HPLC system (LaChrom Elite, Merck-Hitachi, Germany) consisted of an L-2130 pump, an L-2200 autosampler, and an L-2420 UV-VIS detector. EZChrome Elite v. 3.2 (Merck-Hitachi, Germany) computer program was used for data acquisition and integration. The separation of studied compounds was performed using a 250 \times 4.6 mm Supelcosil LC-CN column with a particle size of 5 μm (Sigma-Aldrich, Germany) protected with a guard column (20 \times 4 mm) with the same packing material. The mobile phase consisted of 50 mM potassium dihydrogen phosphate (pH = 4.6), methanol, and acetonitrile mixed at a ratio of 51:40:9, v/v/v and run at 1 mL/min. Chromatographic analysis was carried out at 25 °C and the analytical wavelength was 205 nm.

The calibration curves were constructed by plotting the ratio of peak areas of the studied compound to that of an appropriate IS versus the compound concentration. They were linear in the concentration range of 0.5–5 ng/mL for **56** and 0.25–5 ng/mL for **44** in serum and 1–50 ng/g for **56** and 5–100 ng/g for **44** in brain homogenate. In the case of ultrafiltrate, the calibration curves were linear in the range of 5–700 ng/mL for both compounds. The lower limit of quantification for all biological matrices studied was the lowest calibration standard on the calibration curve, which after extraction procedure was analyzed with a coefficient of variation (CV) of $\leq 20\%$ and a relative error of $\leq 20\%$. No interfering peaks were observed in the chromatograms. The assays were reproducible with low intra- and

inter-day variation (CV < 10%). The concentrations were expressed in ng/mL of serum or ultrafiltrate and ng/g of wet brain tissue.

Determination of *in Vitro* Rat Plasma Protein Binding. Fresh blood was harvested from male adult Wistar rats that were sacrificed by exsanguination. The blood was allowed to clot for 20 min at room temperature and then centrifuged at 3000 rpm for 10 min (Universal 32, Hettich, Germany). **56** and **44** dissolved in water were added in volume of 10 μ L to separate glass tubes containing 1 mL aliquots of rat serum to achieve final concentrations of 3 and 30 μ g/mL each. All tests were run in triplicate. After vortexing, the serum samples were incubated in a water bath at 37 °C for 30 min with gentle shaking. Following this incubation period, 100 μ L of serum samples from each tube were transferred to Eppendorf tubes and frozen at -80 °C for analysis. The remaining serum was transferred into Centrifree ultrafiltration devices with Ultracel regenerated cellulose membrane (Merck, Darmstadt, Germany) and centrifuged at 1000g for 15 min (EBA III centrifuge, Hettich, Germany). The collected ultrafiltrates were frozen (-80 °C) for further analysis.

■ ASSOCIATED CONTENT

Supporting Information

The Supporting Information is available free of charge at <https://pubs.acs.org/doi/10.1021/acs.jmedchem.0c00814>.

Functional activity data with SEM/range values, dose-response curves for functional activity, developability parameters of the target compounds (Fsp3, LELP, CNS-MPO), metabolic stability data, UPLC chromatograms of the reaction mixtures, *in silico* prediction and the proposed structures of metabolites, selectivity of **3**, **44**, and **56** against a broad panel of off-targets, results of the *in vivo* pharmacodynamics studies of **44** and **56**, serum and brain exposure of **44** and **56**, detailed procedures for preparation of the amine intermediates 6–8 and 10–26, and spectra of the target compounds (¹H NMR, ¹⁹F NMR, ¹³C NMR, HPLC) (PDF)

Molecular formula strings (CSV)

■ AUTHOR INFORMATION

Corresponding Author

Marcin Kolaczowski – Faculty of Pharmacy, Jagiellonian University Medical College, 30-688 Kraków, Poland; orcid.org/0000-0001-8402-1121; Phone: (48)12620546; Email: marcin.kolaczowski@uj.edu.pl; Fax: (48)126205458

Authors

Joanna Sniecikowska – Faculty of Pharmacy, Jagiellonian University Medical College, 30-688 Kraków, Poland;

orcid.org/0000-0002-5296-7964

Monika Gluch-Lutwin – Faculty of Pharmacy, Jagiellonian University Medical College, 30-688 Kraków, Poland

Adam Bucki – Faculty of Pharmacy, Jagiellonian University Medical College, 30-688 Kraków, Poland; orcid.org/0000-0003-0451-9814

Anna Więckowska – Faculty of Pharmacy, Jagiellonian University Medical College, 30-688 Kraków, Poland;

orcid.org/0000-0003-2549-170X

Agata Siwek – Faculty of Pharmacy, Jagiellonian University Medical College, 30-688 Kraków, Poland

Magdalena Jastrzebska-Wiesek – Faculty of Pharmacy, Jagiellonian University Medical College, 30-688 Kraków, Poland

Anna Partyka – Faculty of Pharmacy, Jagiellonian University Medical College, 30-688 Kraków, Poland

Daria Wilczyńska – Faculty of Pharmacy, Jagiellonian University Medical College, 30-688 Kraków, Poland

Karolina Pytka – Faculty of Pharmacy, Jagiellonian University Medical College, 30-688 Kraków, Poland

Gniewomir Latacz – Faculty of Pharmacy, Jagiellonian University Medical College, 30-688 Kraków, Poland

Katarzyna Przejczowska-Pomierny – Faculty of Pharmacy, Jagiellonian University Medical College, 30-688 Kraków, Poland

Elżbieta Wyska – Faculty of Pharmacy, Jagiellonian University Medical College, 30-688 Kraków, Poland

Anna Wesołowska – Faculty of Pharmacy, Jagiellonian University Medical College, 30-688 Kraków, Poland

Maciej Pawłowski – Faculty of Pharmacy, Jagiellonian University Medical College, 30-688 Kraków, Poland

Adrian Newman-Tancredi – Neurolixis, Castres, France;

orcid.org/0000-0002-2923-5714

Complete contact information is available at:

<https://pubs.acs.org/10.1021/acs.jmedchem.0c00814>

Author Contributions

All authors have contributed and have given approval to the final version of the manuscript.

Notes

The authors declare the following competing financial interest(s): A.N.-T. is an employee and a shareholder of Neurolixis.

■ ACKNOWLEDGMENTS

This study was financially supported by The National Science Centre (NCN) grant no. 2015/19/B/NZ7/03543.

■ ABBREVIATIONS

SFARs, structure functional activity relationships; cAMP, cyclic adenosine monophosphate; ERK1/2, extracellular signal-regulated kinase 1/2; **1** (F15599), {[1-(3-chloro-4-fluorobenzoyl)-4-fluoropiperidin-4-yl]methyl}[(5-methylpyrimidin-2-yl)methyl]amine; FST, forced swimming test (Porsolt test); LLR, lower lip retraction; IFD, induced fit docking; LLE, lipophilic ligand efficiency; PAINS, pan-assay interference compounds; WAY-100635, N-[2-[4-(2-methoxyphenyl)-piperazin-1-yl]ethyl]-N-pyridin-2-ylcyclohexanecarboxamide; RLMs, rat liver microsomes

■ REFERENCES

- (1) Pazos, A.; Palacios, J. M. Quantitative Autoradiographic Mapping of Serotonin Receptors in the Rat Brain. I. Serotonin-1 Receptors. *Brain Res.* **1985**, *346*, 205–230.
- (2) Fargin, A.; Raymond, J. R.; Lohse, M. J.; Kobilka, B. K.; Caron, M. G.; Lefkowitz, R. J. The Genomic Clone G-21 Which Resembles a β -Adrenergic Receptor Sequence Encodes the 5-HT_{1A} Receptor. *Nature* **1988**, *335*, 358–360.
- (3) Peroutka, S. J. Selective Interaction of Novel Anxiolytics with 5-Hydroxytryptamine_{1A} Receptors. *Biol. Psychiatry* **1985**, *20*, 971–979.
- (4) Jordan, S.; Koprivica, V.; Chen, R.; Tottori, K.; Kikuchi, T.; Altar, C. A. The Antipsychotic Aripiprazole Is a Potent, Partial Agonist at the Human 5-HT_{1A} Receptor. *Eur. J. Pharmacol.* **2002**, *441*, 137–140.
- (5) Adell, A. Lu-AA21004, a Multimodal Serotonergic Agent, for the Potential Treatment of Depression and Anxiety. *IDrugs* **2010**, *12*, 900–910.
- (6) Newman-Tancredi, A.; Cussac, D.; Quentric, Y.; Touzard, M.; Verrière, L.; Carpentier, N.; Millan, M. J. Differential Actions of Antiparkinson Agents at Multiple Classes of Monoaminergic

Receptor. III. Agonist and Antagonist Properties at Serotonin, 5-HT₁ and 5-HT₂, Receptor Subtypes. *J. Pharmacol. Exp. Ther.* **2002**, *303*, 815–822.

(7) Snieciowska, J.; Newman-Tancredi, A.; Kolaczowski, M. From Receptor Selectivity to Functional Selectivity: The Rise of Biased Agonism in 5-HT_{1A} Receptor Drug Discovery. *Curr. Top. Med. Chem.* **2019**, *19*, 2393–2420.

(8) Artigas, F.; Bortolozzi, A.; Celada, P. Can We Increase Speed and Efficacy of Antidepressant Treatments? Part I: General Aspects and Monoamine-Based Strategies. *Eur. Neuropsychopharmacol.* **2018**, *28*, 445–456.

(9) Bologna, Z.; Teoh, J.-P.; Bayoumi, A. S.; Tang, Y.; Kim, I.-M. Biased G Protein-Coupled Receptor Signaling: New Player in Modulating Physiology and Pathology. *Biomol. Ther.* **2017**, *25*, 12–25.

(10) Rodríguez-Espigares, I.; Kaczor, A. A.; Stepniewski, T. M.; Selent, J. Challenges and Opportunities in Drug Discovery of Biased Ligands. *Methods Mol. Biol.* **2018**, *1705*, 321–334.

(11) Seyedabadi, M.; Ghahremani, M. H.; Albert, P. R. Biased Signaling of G Protein Coupled Receptors (GPCRs): Molecular Determinants of GPCR/Transducer Selectivity and Therapeutic Potential. *Pharmacol. Ther.* **2019**, *200*, 148–178.

(12) Newman-Tancredi, A.; Martel, J.-C.; Assié, M.-B.; Buritova, J.; Laouressergues, E.; Cosi, C.; Heusler, P.; Bruins Slot, L.; Colpaert, F.; Vacher, B.; Cussac, D. Signal Transduction and Functional Selectivity of F15599, a Preferential Post-Synaptic 5-HT_{1A} Receptor Agonist. *Br. J. Pharmacol.* **2009**, *156*, 338.

(13) Snieciowska, J.; Gluch-Lutwin, M.; Bucki, A.; Więckowska, A.; Siwek, A.; Jastrzebska-Wiesek, M.; Partyka, A.; Wilczyńska, D.; Pytka, K.; Pocięcha, K.; Cios, A.; Wyska, E.; Wesolowska, A.; Pawlowski, M.; Varney, M. A.; Newman-Tancredi, A.; Kolaczowski, M. Novel Aryloxyethyl Derivatives of 1-(1-Benzoylpiperidin-4-yl)methanamine as the Extracellular Regulated Kinases 1/2 (ERK1/2) Phosphorylation-Preferring Serotonin 5-HT_{1A} Receptor-Biased Agonists with Robust Antidepressant-like Activity. *J. Med. Chem.* **2019**, *62*, 2750–2771.

(14) Becker, G.; Bolbos, R.; Costes, N.; Redouté, J.; Newman-Tancredi, A.; Zimmer, L. Selective Serotonin 5-HT_{1A} Receptor Biased Agonists Elicit distinct Brain Activation Patterns: A PharmacMRI Study. *Sci. Rep.* **2016**, *6*, 26633.

(15) Snieciowska, J.; Newman-Tancredi, A.; Kolaczowski, M. From Receptor Selectivity to Functional Selectivity: The Rise of Biased Agonism in 5-HT_{1A} Receptor Drug Discovery. *Curr. Top. Med. Chem.* **2019**, *19*, 2393–2420.

(16) Newman-Tancredi, A. Biased Agonism at Serotonin 5-HT_{1A} Receptors: Preferential Postsynaptic Activity for Improved Therapy of CNS Disorders. *Neuropsychiatry* **2011**, *1*, 149–164.

(17) Abdala, A. P.; Bissonnette, J. M.; Newman-Tancredi, A. Pinpointing Brainstem Mechanisms Responsible for Autonomic Dysfunction in Rett Syndrome: Therapeutic Perspectives for 5-HT_{1A} Agonists. *Front. Physiol.* **2014**, *5*, 205.

(18) Depoortère, R.; Papp, M.; Gruca, P.; Lason-Tyburkiewicz, M.; Niemczyk, M.; Varney, M. A.; Newman-Tancredi, A. Cortical 5-Hydroxytryptamine 1A Receptor Biased Agonist, NLX-101, Displays Rapid-Acting Antidepressant-like Properties in the Rat Chronic Mild Stress Model. *J. Psychopharmacol.* **2019**, *33*, 1456–1466.

(19) Zhou, Q.; Yang, D.; Wu, M.; Guo, Y.; Guo, W.; Zhong, L.; Cai, X.; Dai, A.; Jang, W.; Shakhnovich, E. I.; Liu, Z.-J.; Stevens, R. C.; Lambert, N. A.; Babu, M. M.; Wang, M.-W.; Zhao, S. Common Activation Mechanism of Class A GPCRs. *eLife* **2019**, *8*, No. e50279.

(20) Williamson, A. Theory of Ætherification. *London Edinburgh Philos. Mag. J. Sci.* **1850**, *37*, 350–356.

(21) Gabriel, S. Ueber Eine Darstellungsweise Primärer Amine Aus Den Entsprechenden Halogenverbindungen. *Ber. Dtsch. Chem. Ges.* **1887**, *20*, 2224–2236.

(22) Wolfe, S.; Hasan, S. K. Five-Membered Rings. II. Inter and Intramolecular Reactions of Simple Amines with N-Substituted Phthalimides. Methylamine as a Reagent for Removal of a Phthaloyl Group from Nitrogen. *Can. J. Chem.* **1970**, *48*, 3572–3579.

(23) Kolaczowski, M.; Marcinkowska, M.; Bucki, A.; Pawlowski, M.; Mitka, K.; Jaśkowska, J.; Kowalski, P.; Kazek, G.; Siwek, A.; Wasik, A.; Wesolowska, A.; Mierzejewski, P.; Bienkowski, P. Novel Arylsulfonamide Derivatives with 5-HT₆/5-HT₇ Receptor Antagonism Targeting Behavioral and Psychological Symptoms of Dementia. *J. Med. Chem.* **2014**, *57*, 4543–4557.

(24) Mitsunobu, O.; Yamada, M.; Mukaiyama, T. Preparation of Esters of Phosphoric Acid by the Reaction of Trivalent Phosphorus Compounds with Diethyl Azodicarboxylate in the Presence of Alcohols. *Bull. Chem. Soc. Jpn.* **1967**, *40*, 935–939.

(25) Mitsunobu, O.; Yamada, M. Preparation of Esters of Carboxylic and Phosphoric Acid via Quaternary Phosphonium Salts. *Bull. Chem. Soc. Jpn.* **1967**, *40*, 2380–2382.

(26) Nowak, M.; Kolaczowski, M.; Pawlowski, M.; Bojarski, A. J. Homology Modeling of the Serotonin 5-HT_{1A} Receptor Using Automated Docking of Bioactive Compounds with Defined Geometry. *J. Med. Chem.* **2006**, *49*, 205–214.

(27) van Wijngaarden, I.; Tulp, M. T. M.; Soudijn, W. The Concept of Selectivity in 5-HT Receptor Research. *Eur. J. Pharmacol.* **1990**, *188*, 301–312.

(28) Hamon, M.; Fattaccini, C. M.; Adrien, J.; Gallissot, M. C.; Martin, P.; Gozlan, H. Alterations of Central Serotonin and Dopamine Turnover in Rats Treated with Ipsapirone and Other 5-Hydroxytryptamine_{1A} Agonists with Potential Anxiolytic Properties. *J. Pharmacol. Exp. Ther.* **1988**, *246*, 745–752.

(29) Foreman, M. M.; Fuller, R. W.; Leander, J. D.; Benvenga, M. J.; Wong, D. T.; Nelson, D. L.; Calligaro, D. O.; Swanson, S. P.; Lucot, J. B.; Flaugh, M. E. Preclinical Studies on LY228729: A Potent and Selective Serotonin_{1A} Agonist. *J. Pharmacol. Exp. Ther.* **1993**, *267*, 58–71.

(30) Harada, K.; Kawaguchi, A.; Ohmori, M.; Fujimura, A. Antagonistic Activity of Tamsulosin against Human Vascular Alpha₁-Adrenergic Receptors. *Clin. Pharmacol. Ther.* **2000**, *67*, 405–412.

(31) Newman-Tancredi, A.; Assié, M.-B.; Martel, J.-C.; Cosi, C.; Slot, L. B.; Palmier, C.; Raully-Lestienne, I.; Colpaert, F.; Vacher, B.; Cussac, D. F15063, a Potential Antipsychotic with D₂/D₃ Antagonist, 5-HT_{1A} Agonist and D₄ Partial Agonist Properties. I. In Vitro Receptor Affinity and Efficacy Profile. *Br. J. Pharmacol.* **2007**, *151*, 237–252.

(32) Brust, T. F.; Hayes, M. P.; Roman, D. L.; Burris, K. D.; Watts, V. J. J. Bias Analyses of Preclinical and Clinical D₂ Dopamine Ligands: Studies with Immediate and Complex Signaling Pathways. *J. Pharmacol. Exp. Ther.* **2015**, *352*, 480–493.

(33) Griffin, M. T.; Figueroa, K. W.; Liller, S.; Ehlert, F. J. Estimation of Agonist Activity at G Protein-Coupled Receptors: Analysis of M₂ Muscarinic Receptor Signaling through Gi/o, Gs, and G15. *J. Pharmacol. Exp. Ther.* **2007**, *321*, 1193–1207.

(34) Ehlert, F. J. On the Analysis of Ligand-Directed Signaling at G Protein-Coupled Receptors. *Naunyn-Schmiedeberg's Arch. Pharmacol.* **2008**, *377*, 549–577.

(35) Rajagopal, S.; Ahn, S.; Rominger, D. H.; Gowen-MacDonald, W.; Lam, C. M.; Dewire, S. M.; Violin, J. D.; Lefkowitz, R. J. Quantifying Ligand Bias at Seven-Transmembrane Receptors. *Mol. Pharmacol.* **2011**, *80*, 367–377.

(36) Stroth, N.; Niso, M.; Colabufo, N. A.; Perrone, R.; Svenningsson, P.; Lacivita, E.; Leopoldo, M. Arylpiperazine Agonists of the Serotonin 5-HT_{1A} Receptor Preferentially Activate CAMP Signaling versus Recruitment of β -Arrestin-2. *Bioorg. Med. Chem.* **2015**, *23*, 4824–4830.

(37) Depoortère, R.; Auclair, A. L.; Bardin, L.; Colpaert, F. C.; Vacher, B.; Newman-Tancredi, A. F15599, a Preferential Post-Synaptic 5-HT_{1A} Receptor Agonist: Activity in Models of Cognition in Comparison with Reference 5-HT_{1A} Receptor Agonists. *Eur. Neuropsychopharmacol.* **2010**, *20*, 641–654.

(38) Dwivedi, Y.; Rizavi, H. S.; Teppen, T.; Sasaki, N.; Chen, H.; Zhang, H.; Roberts, R. C.; Conley, R. R.; Pandey, G. N. Aberrant Extracellular Signal-Regulated Kinase (ERK) 5 Signaling in Hippo-

campus of Suicide Subjects. *Neuropsychopharmacology* **2007**, *32*, 2338–2350.

(39) Yasuno, F.; Suhara, T.; Nakayama, T.; Ichimiya, T.; Okubo, Y.; Takano, A.; Ando, T.; Inoue, M.; Maeda, J.; Suzuki, K. Inhibitory Effect of Hippocampal 5-HT_{1A} Receptors on Human Explicit Memory. *Am. J. Psychiatr.* **2003**, *160*, 334–340.

(40) Luo, Y.; Kuang, S.; Li, H.; Ran, D.; Yang, J. CAMP/PKA-CREB-BDNF Signaling Pathway in Hippocampus Mediates Cyclooxygenase 2-Induced Learning/Memory Deficits of Rats Subjected to Chronic Unpredictable Mild Stress. *Oncotarget* **2017**, *8*, 35558–35572.

(41) Albert, P. R.; Vahid-Ansari, F. The 5-HT_{1A} Receptor: Signaling to Behavior. *Biochimie* **2019**, *161*, 34–45.

(42) Michel, M. C.; Charlton, S. J. Biased Agonism in Drug Discovery-Is It Too Soon to Choose a Path? *Mol. Pharmacol.* **2018**, *93*, 259–265.

(43) Haberzettl, R.; Bert, B.; Fink, H.; Fox, M. A. Animal Models of the Serotonin Syndrome: A Systematic Review. *Behav. Brain Res.* **2013**, *256*, 328–345.

(44) Jastrzębska-Więsek, M.; Partyka, A.; Rychtyk, J.; Śniecikowska, J.; Kolaczowski, M.; Wesolowska, A.; Varney, M. A.; Newman-Tancredi, A. Activity of Serotonin 5-HT_{1A} Receptor Biased Agonists in Rat: Anxiolytic and Antidepressant-like Properties. *ACS Chem. Neurosci.* **2018**, *9*, 1040–1050.

(45) Berendsen, H. H. G.; Bourgondien, F. G. M.; Broekkamp, C. L. E. Role of Dorsal and Median Raphe Nuclei in Lower Lip Retraction in Rats. *Eur. J. Pharmacol.* **1994**, *263*, 315–318.

(46) Celada, P.; Bortolozzi, A.; Artigas, F. Serotonin 5-HT_{1A} Receptors as Targets for Agents to Treat Psychiatric Disorders: Rationale and Current Status of Research. *CNS Drugs* **2013**, *27*, 703–716.

(47) Levigoureux, E.; Vidal, B.; Fieux, S.; Bouillot, C.; Emery, S.; Newman-Tancredi, A.; Zimmer, L. Serotonin 5-HT_{1A} Receptor Biased Agonists Induce Different Cerebral Metabolic Responses: A [¹⁸F]-Fluorodesoxyglucose Positron Emission Tomography Study in Conscious and Anesthetized Rats. *ACS Chem. Neurosci.* **2019**, *10*, 3108–3119.

(48) Vidal, B.; Bolbos, R.; Redouté, J.; Langlois, J.-B.; Costes, N.; Newman-Tancredi, A.; Zimmer, L. Pharmacological MRI to Investigate the Functional Selectivity of 5-HT_{1A} Receptor Biased Agonists. *Neuropharmacology* **2019**, 107867.

(49) Wang, C.; Jiang, Y.; Ma, J.; Wu, H.; Wacker, D.; Katritch, V.; Han, G. W.; Liu, W.; Huang, X.-P.; Vardy, E.; McCorvy, J. D.; Gao, X.; Zhou, X. E.; Melcher, K.; Zhang, C.; Bai, F.; Yang, H.; Yang, L.; Jiang, H.; Roth, B. L.; Cherezov, V.; Stevens, R. C.; Xu, H. E. Structural Basis for Molecular Recognition at Serotonin Receptors. *Science* **2013**, *340*, 610–614.

(50) Bucki, A.; Marcinkowska, M.; Śniecikowska, J.; Więckowski, K.; Pawłowski, M.; Gluch-Lutwin, M.; Gryboś, A.; Siwek, A.; Pytko, K.; Jastrzębska-Więsek, M.; Partyka, A.; Wesolowska, A.; Mierzejewski, P.; Kolaczowski, M. Novel 3-(1,2,3,6-Tetrahydropyridin-4-yl)-1H-Indole-Based Multifunctional Ligands with Antipsychotic-Like, Mood-Modulating, and Procognitive Activity. *J. Med. Chem.* **2017**, *60*, 7483–7501.

(51) Kolaczowski, M.; Bucki, A.; Feder, M.; Pawłowski, M. Ligand-Optimized Homology Models of D1 and D2 Dopamine Receptors: Application for Virtual Screening. *J. Chem. Inf. Model.* **2013**, *53*, 638–648.

(52) Daina, A.; Michielin, O.; Zoete, V. SwissADME: A Free Web Tool to Evaluate Pharmacokinetics, Drug-Likeness and Medicinal Chemistry Friendliness of Small Molecules. *Sci. Rep.* **2017**, *7*, 42717.

(53) Obach, R. S. Prediction of Human Clearance of Twenty-Nine Drugs from Hepatic Microsomal Intrinsic Clearance Data: An Examination of in Vitro Half-Life Approach and Nonspecific Binding to Microsomes. *Drug Metab. Dispos.* **1999**, *27*, 1350–1359.

(54) Latacz, G.; Lubelska, A.; Jastrzębska-Więsek, M.; Partyka, A.; Sobilo, A.; Olejarz, A.; Kucwaj-Brysz, K.; Satała, G.; Bojarski, A. J.; Wesolowska, A.; Kieć-Kononowicz, K.; Handzlik, J. In the Search for a Lead Structure among Series of Potent and Selective Hydantoin 5-

HT_{7R} Agents: The Drug-Likeness in Vitro Study. *Chem. Biol. Drug Des.* **2017**, *90*, 1295–1306.

(55) Latacz, G.; Lubelska, A.; Jastrzębska-Więsek, M.; Partyka, A.; Kucwaj-Brysz, K.; Wesolowska, A.; Kieć-Kononowicz, K.; Handzlik, J. MF-8, a Novel Promising Arylpiperazine-Hydantoin Based 5-HT₇ Receptor Antagonist: In Vitro Drug-Likeness Studies and in Vivo Pharmacological Evaluation. *Bioorg. Med. Chem. Lett.* **2018**, *28*, 878–883.

(56) Cruciani, G.; Carosati, E.; De Boeck, B.; Ethirajulu, K.; Mackie, C.; Howe, T.; Vianello, R. MetaSite: Understanding Metabolism in Human Cytochromes from the Perspective of the Chemist. *J. Med. Chem.* **2005**, *48*, 6970–6979.

(57) Chen, X.; Murawski, A.; Patel, K.; Crespi, C. L.; Balimane, P. V. A Novel Design of Artificial Membrane for Improving the PAMPA Model. *Pharm. Res.* **2008**, *25*, 1511–1520.

(58) Lipinski, C. A.; Lombardo, F.; Dominy, B. W.; Feeney, P. J. Experimental and Computational Approaches to Estimate Solubility and Permeability in Drug Discovery and Development Settings. *Adv. Drug Deliv. Rev.* **2001**, *46*, 3–26.

(59) Hidalgo, I. J.; Raub, T. J.; Borchardt, R. T. Characterization of the Human Colon Carcinoma Cell Line (Caco-2) as a Model System for Intestinal Epithelial Permeability. *Gastroenterology* **1989**, *96*, 736–749.

(60) Obach, R. S.; Baxter, J. G.; Liston, T. E.; Silber, B. M.; Jones, B. C.; MacIntyre, F.; Rance, D. J.; Wastall, P. The Prediction of Human Pharmacokinetic Parameters from Preclinical and in Vitro Metabolism Data. *J. Pharmacol. Exp. Ther.* **1997**, *283*, 46–58.

(61) Banker, M. J.; Clark, T. H.; Williams, J. A. Development and Validation of a 96-Well Equilibrium Dialysis Apparatus for Measuring Plasma Protein Binding. *J. Pharm. Sci.* **2003**, *92*, 967–974.

(62) Stresser, D. M.; Blanchard, A. P.; Turner, S. D.; Erve, J. C.; Dandeneau, A. A.; Miller, V. P.; Crespi, C. L. Substrate-Dependent Modulation of CYP3A4 Catalytic Activity: Analysis of 27 Test Compounds with Four Fluorometric Substrates. *Drug Metab. Dispos.* **2000**, *28*, 1440–1448.

(63) Ono, S.; Hatanaka, T.; Hotta, H.; Satoh, T.; Gonzalez, F. J.; Tsutsui, M. Specificity of Substrate and Inhibitor Probes for Cytochrome P450s: Evaluation of in Vitro Metabolism Using CDNA-Expressed Human P450s and Human Liver Microsomes. *Xenobiotica* **1996**, *26*, 681–693.

(64) Polli, J. W.; Wring, S. A.; Humphreys, J. E.; Huang, L.; Morgan, J. B.; Webster, L. O.; Serabjit-Singh, C. S. Rational Use of in Vitro P-Glycoprotein Assays in Drug Discovery. *J. Pharmacol. Exp. Ther.* **2001**, *299*, 620–628.

(65) Mathes, C. QPatch: The Past, Present and Future of Automated Patch Clamp. *Expert Opin. Ther. Targets* **2006**, *10*, 319–327.

(66) Porsolt, R. D.; Anton, G.; Blavet, N.; Jalfre, M. Behavioural Despair in Rats: A New Model Sensitive to Antidepressant Treatments. *Eur. J. Pharmacol.* **1978**, *47*, 379–391.

(67) Detke, M. J.; Rickels, M.; Lucki, I. Active Behaviors in the Rat Forced Swimming Test Differentially Produced by Serotonergic and Noradrenergic Antidepressants. *Psychopharmacology* **1995**, *121*, 66–72.

(68) Kleven, M. S.; Assié, M. B.; Koek, W. Pharmacological Characterization of in Vivo Properties of Putative Mixed 5-HT_{1A} Agonist/5-HT_{2A/2C} Antagonist Anxiolytics. II. Drug Discrimination and Behavioral Observation Studies in Rats. *J. Pharmacol. Exp. Ther.* **1997**, *282*, 747–759.